

## Article

## Generalized Fractional Bézier Curve with Shape Parameters

Syed Ahmad Aidil Adha Said Mad Zain <sup>1</sup>, Md Yushalify Misro <sup>1,\*</sup> and Kenjiro T. Miura <sup>2</sup><sup>1</sup> School of Mathematical Sciences, Universiti Sains Malaysia, Gelugor 11800, Malaysia; syedaidiladha96@gmail.com<sup>2</sup> Department of Mechanical Engineering, Shizuoka University, Hamamatsu 432-8561, Japan; miura.kenjiro@shizuoka.ac.jp

\* Correspondence: yushalify@usm.my

**Abstract:** The construction of new basis functions for the Bézier or B-spline curve has been one of the most popular themes in recent studies in Computer Aided Geometric Design (CAGD). Implementing the new basis functions with shape parameters provides a different viewpoint on how new types of basis functions can develop complex curves and surfaces beyond restricted formulation. **The wide selection of shape parameters allows more control over the shape of the curves and surfaces without altering their control points.** However, interpolated parametric curves with higher degrees tend to overshoot in the process of curve fitting, making it difficult to control the optimal length of the curved trajectory. Thus, a new parameter needs to be created to overcome this constraint to produce free-form shapes of curves and surfaces while still preserving the basic properties of the Bézier curve. In this work, a general fractional Bézier curve with shape parameters and a fractional parameter is presented. Furthermore, parametric and geometric continuity between two generalized fractional Bézier curves is discussed in this paper, as well as demonstrating the effect of the fractional parameter of curves and surfaces. However, the conventional parametric and geometric continuity can only be applied to connect curves at the endpoints. Hence, a new type of continuity called fractional continuity is proposed to overcome this limitation. Thus, with the curve flexibility and adjustability provided by the generalized fractional Bézier curve, the construction of complex engineering curves and surfaces will be more efficient.

**Keywords:** shape parameters; Riemann-Liouville fractional integral; fractional parameter; parametric and geometric continuity; fractional continuity; fractional Bézier curve



**Citation:** Said Mad Zain, S.A.A.A.; Misro, M.Y.; Miura, K.T. Generalized Fractional Bézier Curve with Shape Parameters. *Mathematics* **2021**, *9*, 2141. <https://doi.org/10.3390/math9172141>

Academic Editor: Ion Mihai

Received: 22 July 2021

Accepted: 27 August 2021

Published: 2 September 2021

**Publisher's Note:** MDPI stays neutral with regard to jurisdictional claims in published maps and institutional affiliations.



**Copyright:** © 2021 by the authors. Licensee MDPI, Basel, Switzerland. This article is an open access article distributed under the terms and conditions of the Creative Commons Attribution (CC BY) license (<https://creativecommons.org/licenses/by/4.0/>).

## 1. Introduction

The Bézier curve is a topic in CAGD that is often discussed because of its geometric properties [1,2]. A classical Bézier curve with Bernstein polynomials as its basis functions become the foundation to develop complex curves and surfaces. The shape of the classical Bézier curve can be altered by changing the control points. However, changing them can affect the continuity and the smoothness of the Bézier curves. Hence, to overcome this limitation, many researchers have introduced the aesthetic Bézier curve with shape parameters by maintaining the classical Bézier curve's properties, thus improving curve flexibility. Yang and Zeng [3] implemented  $n$ th degree of Bézier curve with  $n$  shape parameters. Wang and Wang [4] introduced the general Bézier curve with shape parameters by an integral approach. There are also numerous research in which the basis functions are constructed from trigonometric functions [5–7]. Furthermore, Dube and Sharma [5] constructed the quartic trigonometric with a shape parameter, while Han et al. [6] and Misro et al. [7] introduced the cubic and quintic trigonometric Bézier curve with two shape parameters, respectively. The research on the basis function from Han et al. [6] is extended and applied to the motion study from a straight line to a circle, known as spiral [8,9]. The discussion of the application using a quintic trigonometric Bézier curve as a basis function can be seen in [10,11].

Construction of a basis function for the aesthetic Bézier curve with shape parameters plays an essential role in controlling the shape of the curves. It can be controlled by varying the spectrum value of shape parameters while maintaining its control points. Bézier curves are prominently useful, given their functionality in splicing the curve during subdivision processes, and the curves are able to be interpolated at both endpoints. However, the existing classical or aesthetic Bézier curve tends to overshoot when higher degrees of curves are applied to interpolate or fit numerous points. This drawback is possible to overcome by controlling the optimal length of the curve. To achieve a self-intersection-free curve as in [12,13], all of the examples in this paper show that the objects can be constructed using interpolation Bézier/spline curve. Moreover, by referring to [14], the self-intersection-free curve can also be constructed using different degrees of curves and different levels of continuity. Interpolating the end control points using different degrees of Bézier curve is referred to as hustling. Thus, by embedding the fractional parameter to the curve, the self-intersection-free curve can be constructed by using the same degree of curves. This generalized fractional Bézier curve can be applied in constructing complex engineering curves and surfaces. This new type of basis function can be useful in advanced manufacturing, such as 3D printing.

In CAGD, parametric representation of curves and surfaces is widely used in architecture, shipbuilding, and manufacturing. The constructed curves can be extended to surface modelling. Piegl and Tiller [15] had generated numerous surfaces, such as surface revolution using rational B-spline. Dimas and Briassoulis [16] modelled a few surfaces such as ruled surface, surface revolution, and extruded surface for non-uniform rational basis spline (NURBS). Other examples regarding the surface revolution of Bézier surfaces for some degrees are provided in [17,18]. Biquintic surface with local shape adjustable is also recently developed by [19]. The complexity of curve construction may sometimes cause a delay in the process of curve modelling. This situation can be rectified by using continuity, where complex curves can be broken down into simpler curves before they are connected. Parametric continuity and geometric continuity have become important aspects in the modelling of curves, given its property as an enabler for two curves to connect smoothly. Generally, these two types of continuity are the common measuring standards in constructing smooth curves and surfaces.

DeRose and Barsky [20] has introduced the definition of parametric continuity and geometric continuity for the parametric curve. Ziatdinov et al. [21] used multiple of Log-aesthetic curve (LAC) connected by  $G^2$  continuity to generate C-shaped and applied it in modelling of gear design and railroad track design. Barsky and DeRose [22] discussed the construction of geometric continuity for Bézier curve and Beta spline (B-spline). Some researchers have discussed the  $C^0$ ,  $C^1$  and  $C^2$  continuity and  $G^0$ ,  $G^1$  and  $G^2$  continuity for numerous aesthetic Bézier curves such as the general Bézier (GE-Bézier) curve with  $n$  shape parameters [23] and rational quadratic trigonometric Bézier (RQT-Bézier) with two shape parameters [24]. Quintic trigonometric Bézier curve with two shape parameters [7] and Q-Bézier curve [25] also discussed the same degree of parametric and geometric continuity. Another aesthetic Bézier curve such as general hybrid trigonometric Bézier (GHT-Bézier) curve [26] also discussed parametric continuity and geometric continuity of respective curves up to  $C^3$  and  $G^3$ .

However, there lies a significant limitation in the current continuity concept. Parametric and geometric continuity enables the curves to be connected at two fixed points, which are the endpoints. Thus, if the designer wants to connect at any point of the first curve (for example, the midpoint of the first curve) to the second curve, it can be done by using the subdivision method to splice the first curve and connect the endpoint of the new first curve to the second curve. Nevertheless, this method is tedious, with high computational cost, especially when involving a high degree of curves. Hence, this paper proposes a new type of continuity called fractional continuity to provide an alternative to the subdivision method.

Fractional calculus is the study of differentiation and integration of non-integer order. It is applied in many fields of engineering and science such as diffusive transport, probability, fluid flow and radiology [27]. Samko et al. [28] thoroughly discussed the definitions of fractional calculus and the derivations of fractional integral and fractional derivative. Miller and Ross [27] had comprehensively reviewed its history, definitions and concepts, while Baleanu et al. [29] meticulously discussed the application of fractional calculus in nanotechnology. Many scholars attempted to improve the definitions of fractional integral and fractional derivative. A new definition called Hadamard fractional integral is introduced by Hadamard [30]. Meanwhile, Caputo [31] introduced a new definition of fractional derivative called the Caputo fractional derivative. Recently, Alqahtani [32] used the new Atangana-Baleanu fractional derivative to model groundwater flow within an unconfined aquifer.

There are numerous research about solving fractional differential equation (FDE) using B-spline. Li [33] proposed the numerical solution of fractional differential equations using cubic B-spline wavelet collocation method. Moreover, Arshed [34] approximated solution of super diffusion fourth-order partial differential equations using the quintic B-spline method. On the other hand, Ghomanjani [35] solved fractional optimal control problems and fractional Riccati differential equations numerically by using Bézier curve. Surprisingly, the research discussing the application of fractional calculus in constructing the Bézier curve is uncommon in CAGD. Most of the research applied the B-spline and Bézier curve to solve problems in FDEs. **In this paper, the new curve is constructed by adopting the concept of fractional calculus.** Riemann-Liouville fractional integral will be used as the foundation to develop a new basis function of this curve. This paper will have two important results. The first result is the effect of a new parameter called the fractional parameter on the constructed curve. By using the fractional parameter, a fraction of the curve can be constructed without changing the domain and control points of the curve. Next, the second result is the new type of continuity called the fractional continuity ( $F^r$  for short) is introduced. Some special conditions need to apply to achieve this fractional continuity. It enables the designer to choose the common point of the connected curves to join at any point along the first curve.

The work is organised as follows. In Section 2, the Riemann-Liouville fractional integral definition will be discussed. Then, the basis functions of generalized fractional Bézier curve are constructed, and the properties of the basis functions are shown. In Section 3, the generalized fractional Bézier curve is constructed, and some properties are presented. The geometric effect of the shape parameter, the effect of the fractional parameter and its effect on the arc length of the curve will be demonstrated. In Section 4, parametric continuity and geometric continuity for generalized fractional Bézier curves will be confabulated. In the same section, the new type of continuity called fractional continuity will be introduced. In Section 5, some shapes are modelled using the generalized fractional Bézier curve. Next, in Section 6, some simple surfaces such as surface revolution and extruded surface are generated using the generalized fractional Bézier curve. Last but not least, in Section 7, the conclusion and recommendation for future works are discussed.

## 2. Generalized Fractional Bézier Basis Functions

### 2.1. Riemann-Liouville Fractional Integral

**Definition 1 (Riemann-Liouville fractional integral).** Let  $\text{Re}(v) > 0$ ,  $J$  is the non-negative region and let  $f$  be piecewise continuous on  $J' = (0, \infty)$  and integrable on any sub-interval of  $J = (0, \infty)$ . Then, for  $t > 0$ , the Riemann-Liouville fractional integral of  $f$  of order  $v$  is as follows:

$$D_t^{-v} f(t) = \frac{1}{\Gamma(v)} \int_0^t (t-x)^{v-1} f(x) dx. \quad (1)$$

In this work,  $f(t) = t$  is defined specifically. Using the substitution method and multiple by parts integrations as in [27], then Equation (1) can be simplified as follows:

$$D_t^{-v}(t) = \frac{1}{\Gamma(v+2)} t^{v+1}. \quad (2)$$

Note that  $v$  is the integral order in this definition. In the next subsection, this integral order is called the fractional parameter in the construction of generalized fractional Bézier curve.

## 2.2. The Construction of Generalized Fractional Bézier Basis Function

Using the Riemann-Liouville fractional integral in Definition 1, the generalized fractional Bézier basis function with the shape parameters is defined. It contains fractional parameter  $v$ , where  $v$  is also an integral order in fractional integral as mentioned in Definition 1. The influence of fractional parameters on the construction of Bézier curve will be discussed further in Section 3.3.

**Definition 2** (Generalized fractional Bézier basis functions). For  $t \in [0, 1]$  and  $v \geq 0$ , the following function is defined as generalized fractional Bézier curve basis function of degree  $n$  with  $n$  shape parameters:

$$\begin{aligned} \bar{B}_{i,n}(t) &= B_{i,n}(t) \left( 1 + \frac{a_i}{n-i+1} (1 - D_t^{-v}(t)) + -\frac{a_{i+1}}{i+1} (D_t^{-v}(t)) \right), \\ -(n-i+1) &< a_i < i, \quad a_i = a_{n+1} = 0, \quad i = 0, 1, \dots, n, \end{aligned} \quad (3)$$

where  $B_{i,n}(t) = \binom{n}{i} (1 - D_t^{-v}(t))^{n-i} (D_t^{-v}(t))^i$  and  $D_t^{-v}(t) = \frac{1}{\Gamma(v+2)} t^{v+1}$ . Note that if  $v = 0$ , and  $a_i = 0$  for  $i = 0, 1, \dots, n$ , then the basis functions will become Bernstein basis functions with the degree of  $n$ . The number of shape parameters depend on the degree of generalized fractional Bézier basis functions. For example, if the fractional Bézier basis functions are cubic, then the number of shape parameters are three. Each degree of fractional Bézier will be have one additional parameter called a fractional parameter.

**Remark 1.** In the Riemann-Liouville fractional integral definition, it is clear from the definition stated that  $v > 0$ . However, for the sake of satisfying the degeneracy property,  $v \geq 0$  is defined. The function used in Definition 1, in which  $f(t) = t$  has been defined and the fractional integral operator  $D_t^{-v}(t) = \frac{1}{\Gamma(v+2)} t^{v+1}$ . If  $v = 0$ , then  $D_t^0(t) = t = f(t)$ . The 0th order integral of  $f(t) = t$  is the function itself. Note that Equation (2) is still valid for  $v \geq 0$ .

**Theorem 1** (Generalized fractional Bézier basis function). The generalized fractional basis functions with shape parameters have the following properties:

1. Degeneracy: When  $v = 0$  and  $a_i = 0$  for  $i = 1, 2, \dots, n$ , the basis function become classical Bernstein basis function.
2. Non-negativity:  $\bar{B}_{i,n}(t) \geq 0, i = 0, 1, \dots, n$ .
3. Partition of unity:  $\sum_{i=0}^n \bar{B}_{i,n}(t) = 1$ .
4. Symmetry:  $\bar{B}_{i,n}(t) = \bar{B}_{n-i,n}(1-t), i = 0, 1, \dots, n$  when  $a_i = -a_{n-i+1}$  and  $v = 0$ .

**Proof.** The proof of each properties will be shown as follows:

1. Degeneracy: When  $v = 0$ ,  $D_t^0(t) = t$  and  $a_i = 0$  for  $i = 1, 2, \dots, n$  implies  $y_{i,1} = y_{i,2} = 0$ . Hence,  $\bar{B}_{i,n}(t) = B_{i,n}(t) = \binom{n}{i} (1-t)^{n-i} (t)^i$ . Therefore, the basis functions becomes general Bernstein basis functions.
2. Non-negativity: For any  $v \geq 0$  and  $t \in [0, 1]$ , it is clear that  $0 \leq D_t^{-v}(t) = \frac{1}{\Gamma(v+2)} t^{v+1} \leq 1$ . Then,  $0 \leq D_t^{-v}(t) \leq 1$  implies that  $-1 \leq -D_t^{-v}(t) \leq 0$ . While,  $-1 \leq -D_t^{-v}(t) \leq 0$  implies that  $0 \leq 1 - D_t^{-v}(t) \leq 1$ . Hence,  $B_{i,n}(t) \geq 0$ . Therefore, Equation (3) and  $B_{i,n}(t) \geq 0$  implies that  $\bar{B}_{i,n}(t) \geq 0$ .
3. Partition of unity: Before the main proving, a lemma is proven first in order to prove the partition of unity.

**Lemma 1.**  $\sum_{i=0}^n B_{i,n}(t) = 1$ .

**Proof of Lemma 1.** Note that since  $0 \leq D_t^{-v}(t) \leq 1$ , then the proving is the same as proving the partition of unity property for the Bernstein basis function. Hence,  $\sum_{i=0}^n B_{i,n}(t) = 1$ . Now, we proceed to the main proving. For any value of  $v$  and  $t \in [0, 1]$ , we have

$$\begin{aligned}
 \sum_{i=0}^n \bar{B}_{i,n}(t) &= \sum_{i=0}^n B_{i,n}(t) + \sum_{i=0}^n \left( \frac{a_i}{n-i+1} (1 - D_t^{-v}(t)) \frac{a_{i+1}}{i+1} D_t^{-v}(t) \right) \\
 &= 1 + \sum_{i=0}^n \frac{a_i}{n-i+1} (1 - D_t^{-v}(t)) B_{i,n}(t) - \sum_{i=0}^n \frac{a_{i+1}}{i+1} D_t^{-v}(t) B_{i,n}(t) \\
 &= 1 + \sum_{i=1}^n \frac{a_i}{n-i+1} (1 - D_t^{-v}(t)) B_{i,n}(t) - \sum_{i=0}^{n-1} \frac{a_{i+1}}{i+1} D_t^{-v}(t) B_{i,n}(t) \\
 &= 1 + \sum_{i=1}^n \left( \frac{a_i}{n-i+1} (1 - D_t^{-v}(t)) B_{i,n}(t) - \frac{a_i}{i} D_t^{-v}(t) B_{i-1,n}(t) \right) \\
 &= 1 + \sum_{i=1}^n a_i \left( \frac{1}{n-i+1} (1 - D_t^{-v}(t)) B_{i,n}(t) - \frac{1}{i} D_t^{-v}(t) B_{i-1,n}(t) \right) \\
 &= 1 + \sum_{i=1}^n a_i \left( \frac{1}{n-i+1} (1 - D_t^{-v}(t)) \frac{n!}{(n-i)!i!} (1 - D_t^{-v}(t))^{n-i} (D_t^{-v}(t))^i \right. \\
 &\quad \left. - \frac{1}{i} D_t^{-v}(t) \frac{n!}{(n-i+1)!(i-1)!} (1 - D_t^{-v}(t))^{n-i+1} (D_t^{-v}(t))^{i-1} \right) \\
 &= 1 + \sum_{i=1}^n a_i \left( \frac{n!}{(n-i+1)!(i)!} (1 - D_t^{-v}(t))^{n-i+1} (D_t^{-v}(t))^i \right. \\
 &\quad \left. - \frac{n!}{(n-i+1)!(i)!} (1 - D_t^{-v}(t))^{n-i+1} (D_t^{-v}(t))^i \right) = 1 + \sum_{i=1}^n a_i (0) = 1.
 \end{aligned}$$

4. Symmetry: Since  $a_i = -a_{n-i+1}$  and  $v = 0$ , the basis function become the Bernstein basis function; hence the symmetry properties is satisfied. Note that the symmetry properties will get a partial symmetrical shape when  $v \neq 0$ , but the curve still preserves the same feature of the symmetrical shape, on a different scale. Based on Figures 1 and 2, it can be observed that the symmetry properties are in full shape when  $a_i = -a_{n-i+1}$  and  $v = 0$ . This new property is further discussed in Section 3.

□

From Definition 2, the number of shape parameters depends on the degree of the curve. Figures 1 and 2 show the graph multiple degrees of fractional Bézier basis functions with multiple values of shape parameters and a fractional parameter. Figure 1 shows the quadratic and cubic fractional Bézier basis functions with shape and fractional parameters. Figure 1a,c,e are the quadratic fractional Bézier basis function of two shape parameters  $(a_1, a_2)$  with  $v = 0, 0.5, 1$ , respectively. On the other hand, Figure 1b,d,f are the cubic fractional Bézier basis function of three shape parameters  $(a_1, a_2, a_3)$  with  $v = 0, 0.5, 1$ , respectively.

The graph of quartic and quintic fractional Bézier basis functions with shape parameters and fractional parameter are shown in Figure 2. The quartic fractional Bézier basis function of four shape parameters  $(a_1, a_2, a_3, a_4)$  with  $v = 0, 0.5, 1$ , respectively are shown in Figure 2a,c,e. On the other hand, Figure 2b,d,f show the quintic fractional Bézier basis function of five shape parameters  $(a_1, a_2, a_3, a_4, a_5)$  with  $v = 0, 0.5, 1$ , respectively.



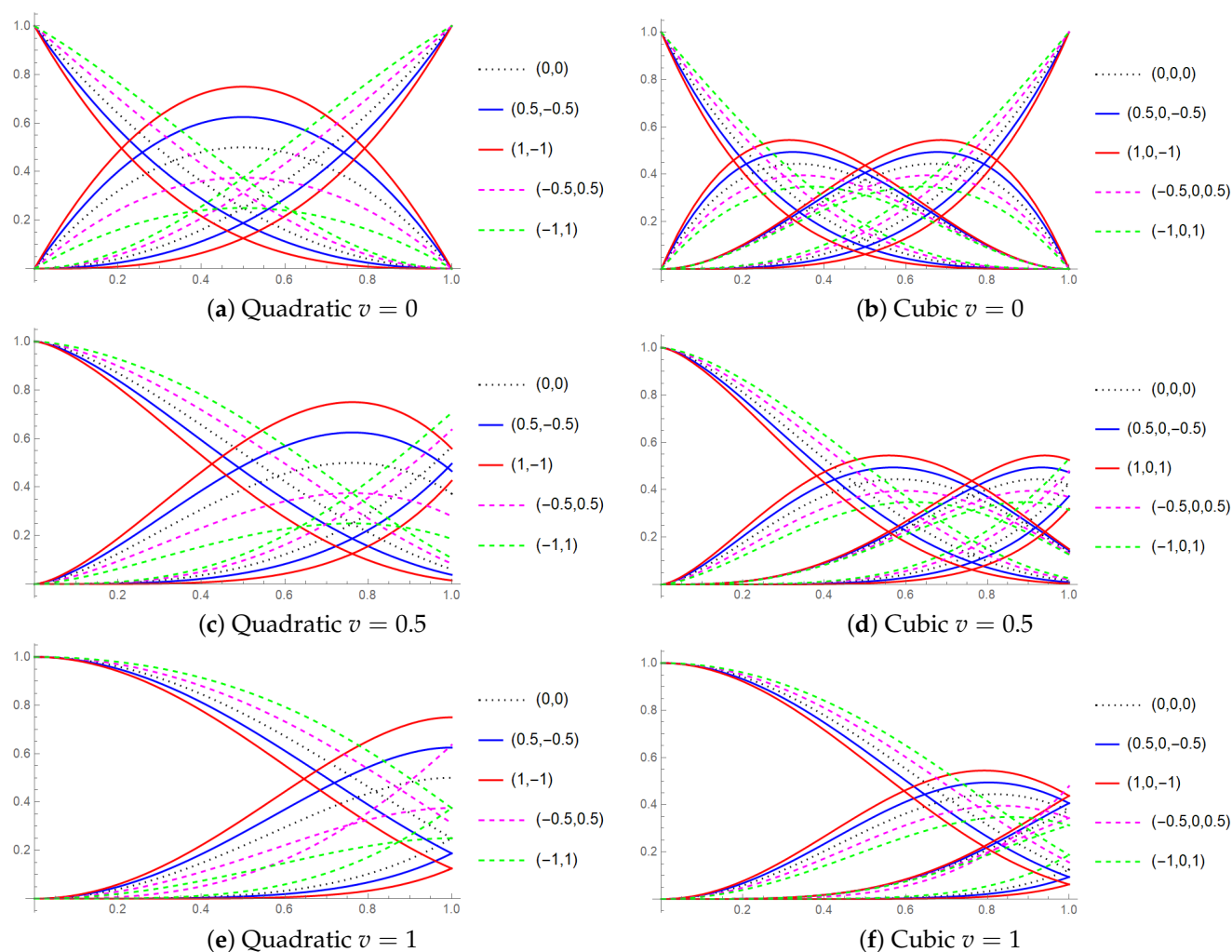


Figure 1. Quadratic and cubic fractional Bézier basis functions with multiple values of  $v$  and shape parameters.

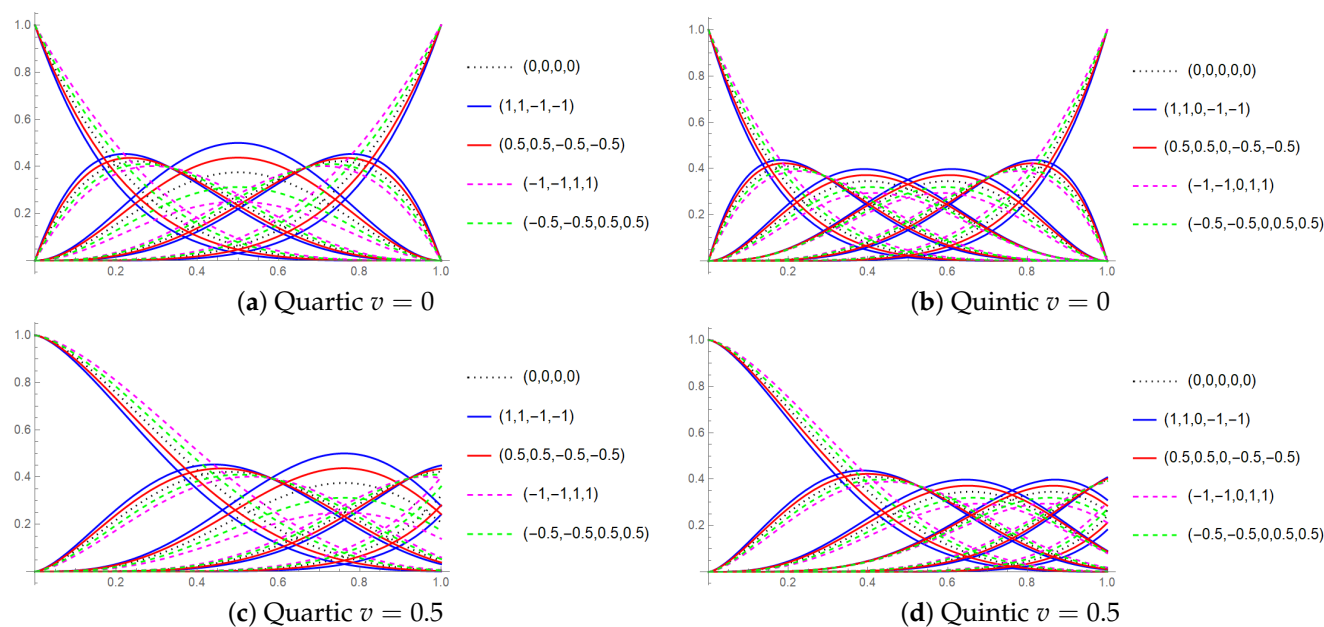


Figure 2. Cont.

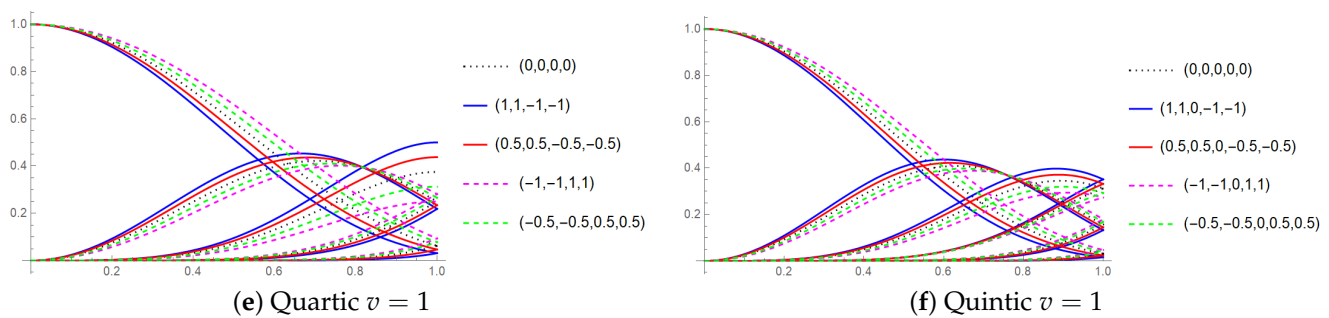


Figure 2. Quartic and quintic fractional Bézier basis functions with multiple values of  $v$  and shape parameters.

### 3. Construction of Generalized Fractional Bézier Curve with Shape Parameters

**Definition 3** (Generalized fractional Bézier curve). *The generalized fractional Bézier curve of  $n$  degree with  $n$  shape parameters is defined as follows:*

$$f(t; v, a_1, a_2, \dots, a_n) = \sum_{i=0}^n \bar{B}_{i,n}(t; v, a_1, a_2, \dots, a_n) P_i, \quad t \in [0, 1], \quad (4)$$

where  $v \geq 0$ ,  $P_i$  for  $i = 0, 1, \dots, n$  is the set of control point in  $\mathbb{R}^m$ ,  $a_0 = a_{n+1} = 0$  and a few terms are defined below:

$$\begin{aligned} \bar{B}_{i,n}(t; v, a_1, a_2, \dots, a_n) &= B_{i,n}(t) \left( 1 + \frac{a_i}{n-i+1} (1 - D_t^{-v}(t)) - \frac{a_{i+1}}{i+1} (D_t^{-v}(t)) \right), \\ B_{i,n}(t) &= \binom{n}{i} (1 - D_t^{-v}(t))^{n-i} (D_t^{-v}(t))^i, \\ D_t^{-v}(t) &= \frac{1}{\Gamma(v+2)} t^{v+1}. \end{aligned}$$

Note that the number of shape parameters depends on the degree of the curve. The higher the degree of curve, the higher the number of shape parameters embedded in the basis function. For each degree of curve, the number of the fractional parameter is always one.

#### 3.1. Properties of Curve

**Theorem 2** (Properties of generalized fractional Bézier curve). *The generalized fractional Bézier curve of degree  $n$  with  $n$  shape parameters has the following properties:*

1. Endpoint terminal
2. Endpoint tangent
3. Convex hull
4. Geometric invariance
5. Shape adjustable property
6. Fractional curve adjustable property

**Proof.** The proof for each properties are as follows:

1. Endpoint terminal:

For any value of  $v \geq 0$  and any degree of  $n$ , the endpoint terminal property is satisfied:

$$\begin{aligned} f(0; v, a_1, a_2, \dots, a_n) &= \sum_{i=0}^n \bar{B}_{i,n}(0; v, a_1, a_2, \dots, a_n) P_i = P_0, \\ f(1; v, a_1, a_2, \dots, a_n) &= \sum_{i=0}^n \bar{B}_{i,n}(1; v, a_1, a_2, \dots, a_n) P_i. \end{aligned} \quad (5)$$

For  $f(1; v, a_1, a_2, \dots, a_n)$ , the endpoint terminal will become the linear combination of  $P_i$ , where  $i = 0, 1, \dots, n$ . Note that when  $v = 0$ , then  $f(1; 0, a_1, a_2, \dots, a_n) = P_n$ . At  $t = 0$ , the endpoint does not depend on the fractional parameter given in Equation (5). However, at  $t = 1$ , the endpoint is not fixed by its last control point as any normal Bézier curve. This implies that the endpoint for fractional Bézier curve at  $t = 1$  depends on the fractional parameter  $v$ . The coordinate of endpoint terminal can be obtained easily using Equation (5) by simply plugging in the value of fractional parameter  $v$ , where the specific coordinate of the endpoint at  $t = 1$  can be determined. This endpoint terminal property for the fractional Bézier curve will provide the particle path that is tractable when the value of  $v$  varies. Hence, the endpoint terminal property is satisfied.

### 2. Endpoint tangent:

This endpoint tangent property is satisfied for  $v \geq 0$ . The values of the endpoint tangent are:

$$f'(0; v, a_1, a_2, \dots, a_n) = (n + a_1)(P_1 - P_0),$$

$$f'(1; v, a_1, a_2, \dots, a_n) = \sum_{i=0}^n \left( \frac{d}{dt} \bar{B}_{i,n}(t; v, a_1, a_2, \dots, a_n) \Big|_{t=1} \right) P_i. \quad (6)$$

For the endpoint tangent at  $t = 0$ , the tangent is not affected by fractional parameter  $v$ . Different values of  $v$  will determine the coordinate of the endpoint terminal for  $t = 1$ . Therefore, the endpoint tangent for  $t = 1$  depends on the value of  $v$ . By having this unique property of fractional parameter, the basis function will provide the optimal length of the curve so that the trajectory of the curve can be controlled. The desired length of the curve can be arbitrarily chosen when  $v \geq 0$ . Special case occur for endpoint at  $t = 1$  when  $v = 0$ , then the endpoint tangent  $f'(1; 0, a_1, a_2, \dots, a_n) = (n - a_n)(P_n - P_{n-1})$ . Hence, the endpoint tangent property is satisfied.

### 3. Convex hull:

In Theorem 2.1, the generalized fractional Bézier basis functions satisfy the partition of unity and non-negativity properties. Hence, the generalized fractional Bézier curve with  $P_i$ , where  $i = 0, 1, \dots, n$  constructed, must lie inside the control polygon as shown in Figures 3–5.

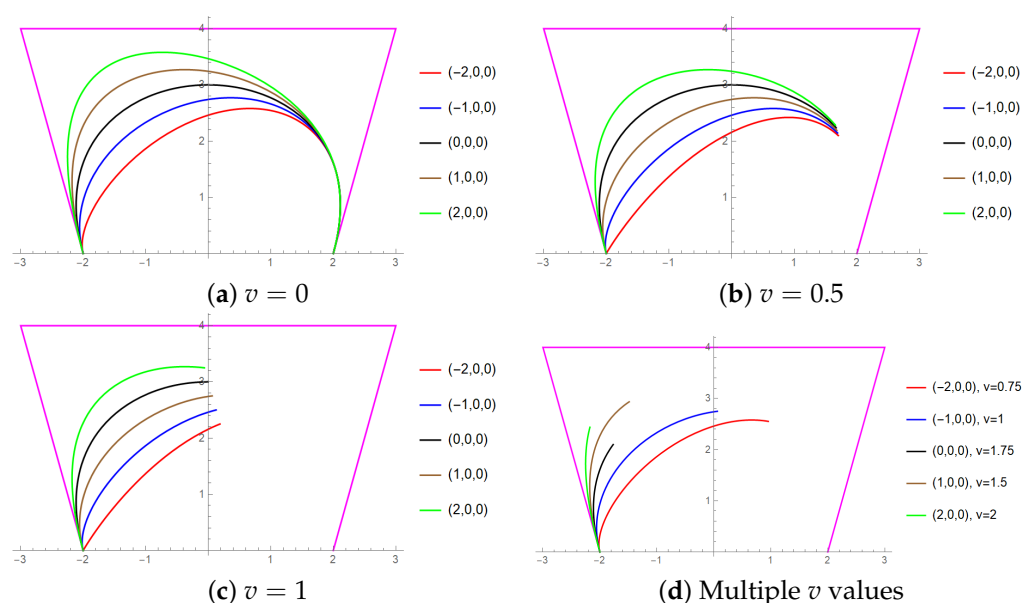
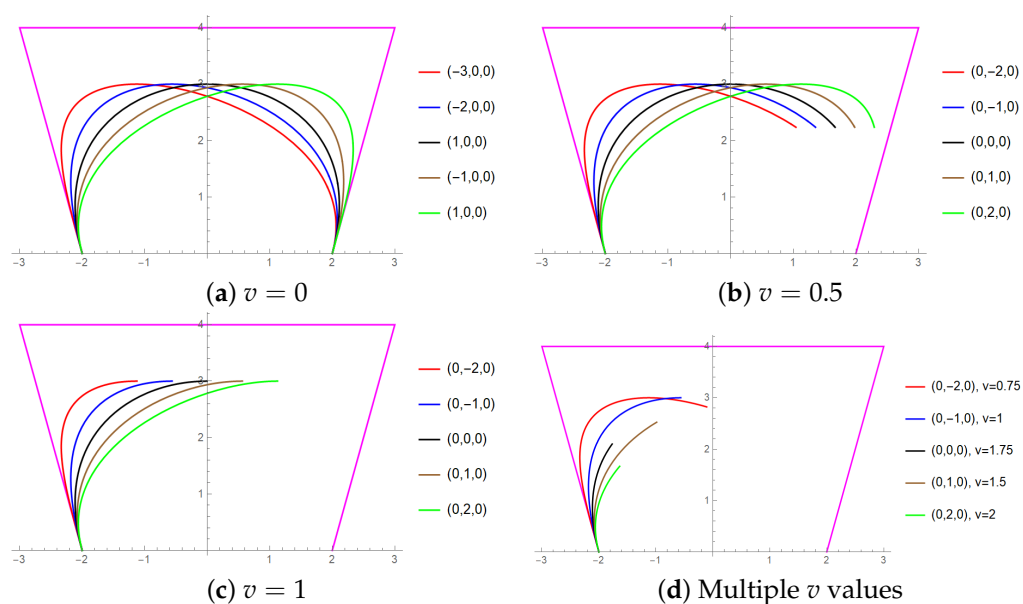
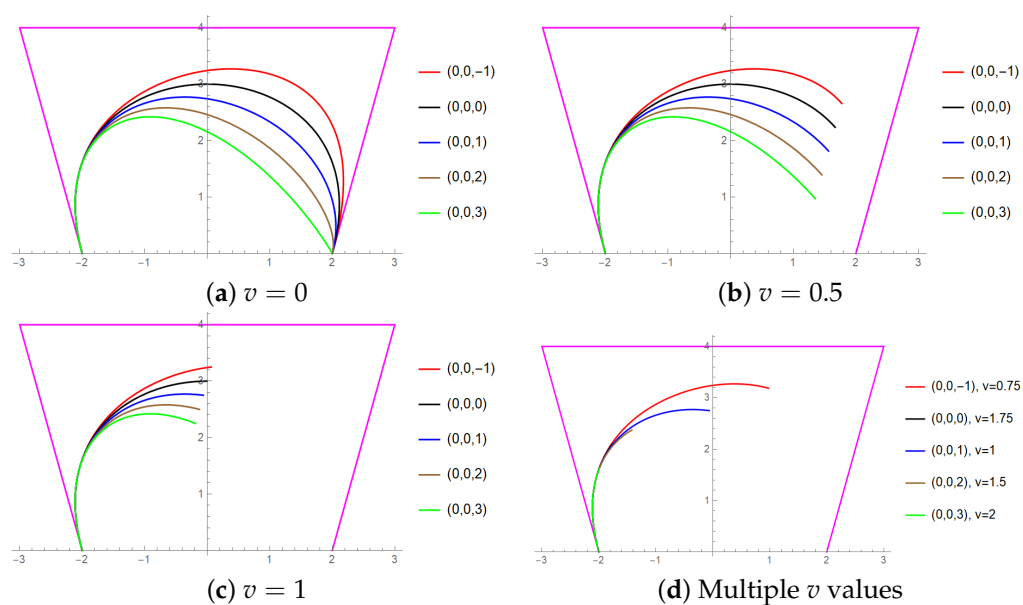


Figure 3. Cubic fractional Bézier curve with multiple values of  $v$  and  $a_1$  shape parameter.





**Figure 4.** Cubic fractional Bézier curve with multiple values of  $v$  and  $a_2$  shape parameter.



**Figure 5.** Cubic fractional Bézier curve with multiple values of  $v$  and  $a_3$  shape parameter.

4. Geometric invariance:

Supposed  $\tilde{K}$  is an arbitrary vector in  $\mathbb{R}^2$  or  $\mathbb{R}^3$  and  $L$  is an arbitrary matrix with size  $l \times l$  for  $l = 2, 3$ , then the following equation is satisfied:

$$\begin{aligned}
 f(t; v, a_1, a_2, \dots, a_n; P_0 + \tilde{K}, P_1 + \tilde{K}, \dots, P_n + \tilde{K}) \\
 = f(t; v, a_1, a_2, \dots, a_n; P_0, P_1, \dots, P_n) + \tilde{K}, \\
 f(t; v, a_1, a_2, \dots, a_n; LP_0, LP_1, \dots, LP_n) \\
 = Lf(t; v, a_1, a_2, \dots, a_n; P_0, P_1, \dots, P_n).
 \end{aligned} \tag{7}$$

(a)

$$\begin{aligned}
f(t; v, a_1, a_2, \dots, a_n; P_0 + \tilde{K}, P_1 + \tilde{K}, \dots, P_n + \tilde{K}) &= \sum_{i=0}^n \tilde{B}_{i,n}(t; v, a_1, a_2, \dots, a_n) P_i \\
&+ \sum_{i=0}^n \tilde{B}_{i,n}(t; v, a_1, a_2, \dots, a_n) \tilde{K} \\
&= f(t; v, a_1, a_2, \dots, a_n; P_0, P_1, \dots, P_n) \\
&+ \tilde{K} \sum_{i=0}^n \tilde{B}_{i,n}(t; v, a_1, a_2, \dots, a_n) \\
&= f(t; v, a_1, a_2, \dots, a_n; P_0, P_1, \dots, P_n) \\
&+ \tilde{K}.
\end{aligned}$$

(b)

$$\begin{aligned}
f(t; v, a_1, a_2, \dots, a_n; LP_0, LP_1, \dots, LP_n) &= \sum_{i=0}^n \tilde{B}_{i,n}(t; v, a_1, a_2, \dots, a_n) (P_i)(L) \\
&= L \sum_{i=0}^n \tilde{B}_{i,n}(t; v, a_1, a_2, \dots, a_n) (P_i) \\
&= Lf(t; v, a_1, a_2, \dots, a_n; P_0, P_1, \dots, P_n).
\end{aligned}$$

### 5. Shape adjustable property:

The classical Bézier curve is a fixed curve within the control polygon. The limitation of the classical Bézier curve is that the curve cannot be altered without changing the control points. The generalized fractional Bézier basis functions with shape parameters can overcome this limitation. The number of shape parameters constructed depends on the number of degrees. Here, the  $n$ -th degree of the curve will have  $n$  number of shape parameters. By using shape parameters, the curve is more flexible without changing the control points.

### 6. Fractional curve adjustable property:

By applying the Riemann-Liouville fractional integral definition in the construction of the Bézier curve, a new parameter called fractional parameter is created. This fractional parameter is used for adjusting and controlling the length of the constructed curve. This property is further discussed in Section 3.3.

□

### 3.2. The Geometric Effect of Shape Parameter on the Curve

In recent years, embedding shape parameters in the Bézier basis functions has become one of the main focuses in CAGD. This is due to the usefulness of shape parameters in enabling the curve to alter its shape without changing any control points while still preserving the properties of the Bézier curve. For the generalized fractional Bézier curve, there is also shape parameters embedded in the basis functions. The number of shape parameters depends on the degree of the curve. The generalized fractional Bézier curve has degree  $n$  if and only if the basis functions have  $n$  shape parameters. Generally, at the endpoint of the curve, there is one shape parameter associated, while the intermediate control points are associated with two shape parameters. Thus, each shape parameter will be associated with two control points. Generally, a shape parameter will be associated with control points  $P_{n-1}$  and  $P_n$  for  $n = 1, 2, \dots, n$ .

Figures 3–5 show a cubic fractional Bézier curve with three shape parameters. In Figures 3–5, shape parameters  $a_1$ ,  $a_2$  and  $a_3$  are changed, respectively. The shape parameters  $a_1$  is associated with  $P_0$  and  $P_1$ . Meanwhile,  $a_2$  will affect the control points  $P_1$  and  $P_2$  and lastly  $a_3$  will integrate with control points  $P_2$  and  $P_3$ . Based on the Figures 3–5, increasing the value  $a_1$ , will cause curve to move closer to the control point  $P_1$ . This effect is also

the same as  $a_2$  and  $a_3$ , as increasing each value, the curve will move closer to  $P_2$  and  $P_3$  respectively. In the next subsection, the effect of the fractional parameter will be discussed.

### 3.3. The Effect of Fractional Parameter on the Curve

In the construction of curve fitting using the Bézier curve, an issue arises where the curve tends to overshoot when a higher degree of curve is used to interpolate the numbers of points. Here, it gets worse when the points are close to each other. Therefore, the generalized fractional Bézier curve with shape parameters has a new parameter called fractional parameter,  $v$ . Using the same control points, the length of the curve is adjustable by varying the fractional parameter  $v$ . Hence, fractional parameter and shape parameters give more control for users to construct the desired curve in terms of shape and length flexibility of the curve. At the same time still, it also preserves the basic properties of Bézier curve. An example is presented below to show the effect of the fractional parameter. A cubic fractional Bézier curve with four control points can be defined as follows:

$$f(t; v, a_1, a_2, a_3) = \sum_{i=0}^3 \bar{B}_{i,3}(t; v, a_1, a_2, a_3) P_i, \quad t \in [0, 1],$$

where  $P_i$  are the control points for  $i = 0, 1, 2, 3$ .

**Example 1.** The control points are  $P_0 = (-2, 0)$ ,  $P_1 = (-3, 4)$ ,  $P_2 = (3, 4)$  and  $P_3 = (2, 0)$  and the curve constructed with different values of shape parameter  $a_1$  and  $v$ . Figures 3–5 show the variation of generalized fractional Bézier curve with different values of shape parameters and fractional parameter.

Figure 3a–c are the cubic fractional Bézier curve with shape parameters as stated in the figures with  $v = 0, 0.5, 1$ , respectively. Figure 3d is the curve with the same shape parameters but with multiple  $v$  values of fractional parameters. Figures 4 and 5 are the same curve with the same control points and fractional parameter as Figure 3, but different shape parameters.

Note that by setting the value of  $v = 0$  and  $a_1 = a_2 = a_3 = 0$ , the generalized fractional Bézier curve becomes classical Bézier curve. The black curve is the classical Bézier curve in Figures 3–5. By observing the figures, a fraction of the curve can be constructed by varying the fractional parameter without changing control points while maintaining the same domain of  $t \in [0, 1]$ .

### 3.4. Fractional De Casteljau Algorithm

The generalized fractional Bézier basis functions can be constructed using the proposed fractional De Casteljau algorithm. The recursive algorithm is the same as the De Casteljau's Algorithm but with some special conditions. The algorithm is as follows:

$$\begin{cases} P_i^0 = P_i, \quad i = 0, 1, \dots, n, \\ P_i^1 = P_i^0(1 - D_t^{-v}(t))(1 - a_{i+1}D_t^{-v}(t)) + P_{i+1}^0D_t^{-v}(t)(1 + a_{i+1}(1 - D_t^{-v}(t))), \\ i = 0, 1, \dots, n-1, \\ P_i^r = P_i^{r-1}(1 - D_t^{-v}(t)) + P_{i+1}^{r-1}D_t^{-v}(t), \\ i = 0, 1, \dots, n, \quad r = 2, 3, \dots, n-r. \end{cases} \quad (8)$$

Then

$$f(t; v, a_1, a_2, \dots, a_n) = \sum_{i=0}^{n-1} P_i^1 = \dots = \sum_{i=0}^{n-r} P_i^{n-r} = \dots = P_0^n. \quad (9)$$

If the shape parameters are set to 0 and  $v = 0$ , the algorithm will revert to the classical De Casteljau algorithm. For simplicity, the quadratic case will be shown. To extension up to the  $n$  degrees general case can be done using induction.

For  $n = 2$ ,

$$P_0^1 = P_0^0(1 - D_t^{-v}(t))(1 - a_1 D_t^{-v}(t)) + P_1^0 D_t^{-v}(t)(1 + a_1(1 - D_t^{-v}(t))), \quad (10)$$

$$P_1^1 = P_1^0(1 - D_t^{-v}(t))(1 - a_2 D_t^{-v}(t)) + P_2^0 D_t^{-v}(t)(1 + a_2(1 - D_t^{-v}(t))). \quad (11)$$

By substituting two previous equations, the quadratic fractional Bézier curve can be derived.

$$\begin{aligned} P_0^2 &= P_0^1(1 - D_t^{-v}(t)) + P_1^1 D_t^{-v}(t) \\ &= P_0^0(1 - D_t^{-v}(t))(1 - a_1 D_t^{-v}(t)) + P_1^0 D_t^{-v}(t)(1 + a_1(1 - D_t^{-v}(t))(1 - D_t^{-v}(t))) \\ &\quad + P_2^0(1 - D_t^{-v}(t))(1 - a_2 D_t^{-v}(t)) + P_2^0 D_t^{-v}(t)(1 + a_2(1 - D_t^{-v}(t)) D_t^{-v}(t)) \\ &= P_0^0(1 - D_t^{-v}(t))^2(1 - a_1 D_t^{-v}(t)) \\ &\quad + 2P_1^0(1 - D_t^{-v}(t)) D_t^{-v}(t) \left(1 + \frac{a_1}{2}(1 - D_t^{-v}(t)) - \frac{a_2}{2} D_t^{-v}(t)\right) \\ &\quad + P_2^0 D_t^{-v}(t)^2 \left(1 + \frac{a_2}{2}(1 - D_t^{-v}(t))\right) \\ &= \sum_{i=0}^n \bar{B}_{i,n}(t; v, a_1, a_2, \dots, a_n) P_i \\ &= P_0^2 = f(t; v, a_1, a_2). \end{aligned}$$

For clear understanding, the fractional De Casteljau Algorithm can be represented by the triangular scheme as shown in Figure 6.

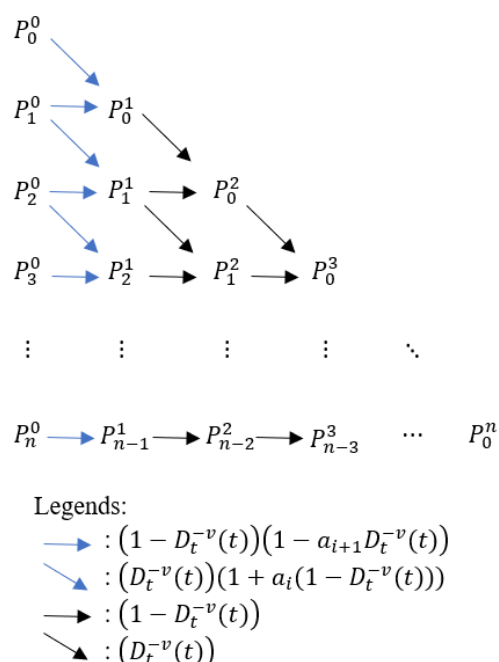


Figure 6. Fractional De Casteljau Algorithm Triangle Scheme.

### 3.5. Arc Length for Generalized Fractional Bézier Curve

Generally, the arc length of a curve is the distance between two points along the curve. In this section, the effect of shape parameters and fractional continuity on the arc length is discussed.

**Definition 4** (Arc length for generalized fractional Bézier curve). Suppose  $f(t; v, a_1, a_2, \dots, a_n)$  be the generalized fractional Bézier curve on  $t \in [0, 1]$ . Then, the arc length is defined as follows:

$$L = \int_0^1 |f'(t; v, a_1, a_2, \dots, a_n)| dt. \quad (12)$$

**Example 2.** Figure 7 shows the cubic fractional Bézier curves with shape parameters. The curves that have low opacity show the original Bézier curves when fractional parameter  $v = 0$ . The magenta curve has shape parameter of  $(0.75, 0.25, -0.8)$ , the black curve has shape parameter of  $(0, 0, 0)$  and the red curve has shape parameter of  $(-0.6, -0.1, 0.9)$ . The solid line shows the cubic fractional at the specific value of fractional parameter  $v$  as stated in the similar figure. Table 1 shows the numerical value of the arc length for Figure 7.

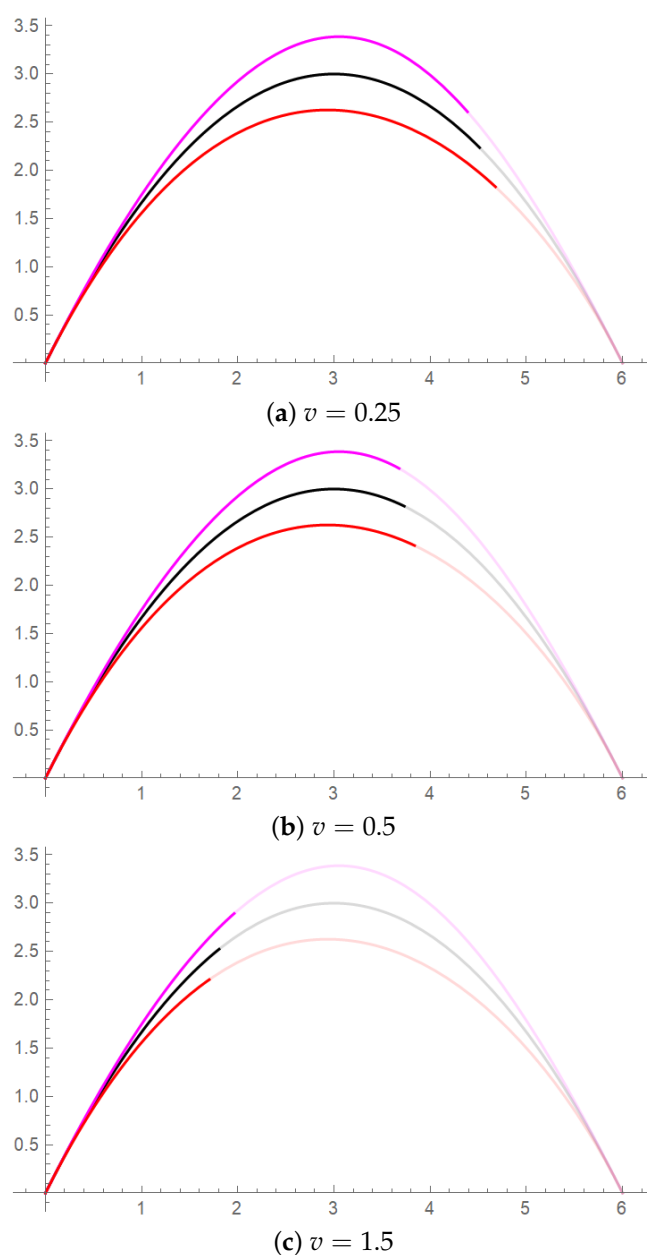


**Figure 7.** Cubic fractional Bézier curve with different fractional parameter and shape parameters.

**Table 1.** The numerical value of arc length for cubic fractional Bézier curve.

Shape Parameters, $(a_1, a_2, a_3)$	Fractional Parameter, $v$	Arc Length
(0, 0, 0) Black	0	8.8737
	0.25	7.4439
	0.5	6.1777
	1.5	3.1259
(0.75, 0.25, −0.8) Magenta	0	9.4246
	0.25	9.4064
	0.5	6.3326
	1.5	3.5155
(−0.6, −0.1, 0.9) Red	0	8.3703
	0.25	7.2651
	0.5	6.1023
	1.5	2.8168

From Figure 7 and Table 1, the higher the value of the fractional parameter, the lower the value of arc length of the curve. This is due to the fractional parameter enabling the user to control the adaptability length of the constructed curve. The shape parameters can be used to the control projection of the arc length. However, the shape parameters have more a restrictive range while the fractional parameter's range is broader since  $v \geq 0$ .

#### 4. Continuity for Generalized Fractional Bézier Curve

In CAGD, some of the constructed curves are too complex. One of the ways to overcome the limitation is to split the curve into a few simple curves. By using continuity, a higher-order of the curve is not needed to construct the complex curve.

##### 4.1. Parametric Continuity for Generalized Fractional Bézier Curve, $C^r$

Parametric continuity is the simplest way to connect between two curves. The parametric continuity must be satisfied in order to connect two simple curves for constructing the desired shape. Continuity is crucial to guarantee the smoothness of the curve [36].

**Definition 5** (General parametric continuity,  $C^r$  for curves). Consider two curves  $x_1$  on  $t \in [a, b]$  and  $x_2$  on  $t \in [a^*, b^*]$  with both curves have a degree of at least  $r + 1$ . The two curves are  $C^r$  continuous if the following condition is satisfied:

$$x_1^{(k)}(b) = x_2^{(k)}(a^*), \quad k = 0, 1, \dots, r. \quad (13)$$

Now, the parametric continuity for the generalized fractional Bézier curve will be discussed. Consider two adjacent generalized fractional Bézier curves as follows:

$$x_1(t; v_1, a_1, a_2, \dots, a_n) = \sum_{i=0}^n \bar{B}_{i,n}(t; v_1, a_1, a_2, \dots, a_n) Q_i, \quad t \in [0, 1], n \geq 3, \quad (14)$$

$$x_2(t; v_2, b_1, b_2, \dots, b_m) = \sum_{j=0}^m \bar{B}_{j,m}(t; v_2, b_1, b_2, \dots, b_m) R_j, \quad t \in [0, 1], m \geq 3, \quad (15)$$

where  $\bar{B}_{i,n}$  and  $\bar{B}_{j,m}$  are generalized fractional Bézier basis functions of degree  $n$  and  $m$ , respectively. The coefficients  $a_1, a_2, \dots, a_n$  and  $b_1, b_2, \dots, b_m$  are the shape parameters. Moreover,  $Q_i (i = 0, 1, \dots, n)$  and  $R_j (j = 0, 1, \dots, m)$  are the control points, while  $v_1$  and  $v_2$  are fractional parameters for  $x_1$  and  $x_2$ , respectively.



**Theorem 3** (Parametric continuity for generalized fractional Bézier curve). Consider two same degrees of generalized fractional Bézier curves as in Equations (14) and (15), the necessary and sufficient conditions for parametric continuity at the joint points of  $v_1 = v_2 = 0$  are given by:

1.  $C^0$  continuity:

$$R_0 = Q_n. \quad (16)$$

2.  $C^1$  continuity:

$$\begin{aligned} R_0 &= Q_n, \\ R_1 &= \frac{(a_n - n)Q_{n-1} + (n - a_n)Q_n + R_0(b_1 + n)}{b_1 + n}. \end{aligned} \quad (17)$$

3.  $C^2$  continuity:

$$\begin{aligned} R_0 &= Q_n, \\ R_1 &= \frac{(a_n - n)Q_{n-1} + (n - a_n)Q_n + R_0(b_1 + n)}{b_1 + n}, \\ R_2 &= \frac{1}{b_2 + n - 1} \left( (-a_{n-1} + n - 1)Q_{n-2} + (a_{n-1} + 2a_n - 2n + 2)Q_{n-1} \right. \\ &\quad \left. - 2a_nQ_n - 2b_1R_0 + 2b_1R_1 + b_2R_1 + nQ_n - Q_n - nR_0 + 2nR_1 + R_0 - 2R_1 \right). \end{aligned} \quad (18)$$

**Proof.** The proof of the theorem is shown as follows:

1. Since  $C^0$  is position continuity, hence common point of the two curves to connect should be decided. In this case, the endpoint of the first curve,  $x_1$ , is connected to the first point of the second curve,  $x_2$ . Hence, by solving  $x_1(1) = x_2(0)$ ,  $C^0$  continuity condition will be satisfied.
2.  $C^0$  continuity condition must be satisfied first.  $C^1$  continuity is tangent continuity at the common point. By solving  $x_1(1) = x_2(0)$  and  $x'_1(1) = x'_2(0)$ , continuity condition of  $C^1$  can be satisfied.
3.  $C^2$  continuity is curvature continuity at the common point. By solving  $x_1(1) = x_2(0)$ ,  $x'_1(1) = x'_2(0)$ , and  $x''_1(1) = x''_2(0)$ ,  $C^0$  and  $C^1$  conditions must be satisfied first in order for  $C^2$  continuity to be satisfied.

□

**Example 3.** Figure 8 shows the cubic fractional Bézier curves with variations of fractional parameters which satisfy the  $C^0$  continuity conditions at their joints.  $a_i$  and  $b_j$  for  $i, j = 1, 2, 3$  are the shape parameters for two adjacent cubic fractional Bézier curves  $x_1(t; v_1, a_1, a_2, a_3)$  and  $x_2(t; v_2, b_1, b_2, b_3)$ , respectively. The control points are  $Q_0 = (0, 0)$ ,  $Q_1 = (2, 4)$ ,  $Q_2 = (4, 4)$  and  $Q_3 = (6, 0)$ . The control point of  $R_0$  and can be obtained by Theorem 3.  $R_1$ ,  $R_2$  and  $R_3$  control points are up to designer choice but for this example,  $R_1 = (7, -5)$ ,  $R_2 = (10, -4)$  and  $R_3 = (12, 0)$  are chosen. The shape parameters used are  $(a_1, a_2, a_3, b_1, b_2, b_3) = (1, 0, -1, 1, 0.5, 2)$ . The fractional Bézier curve can always be converted to an ordinary Bézier curve when  $v_2 = 0$ , as shown in Examples 4 and 5. In these examples, the second curve has two different lines, one with a solid line and another one with opacity. The opacity line is represented by the ordinary Bézier curve when  $v_2 = 0$ .

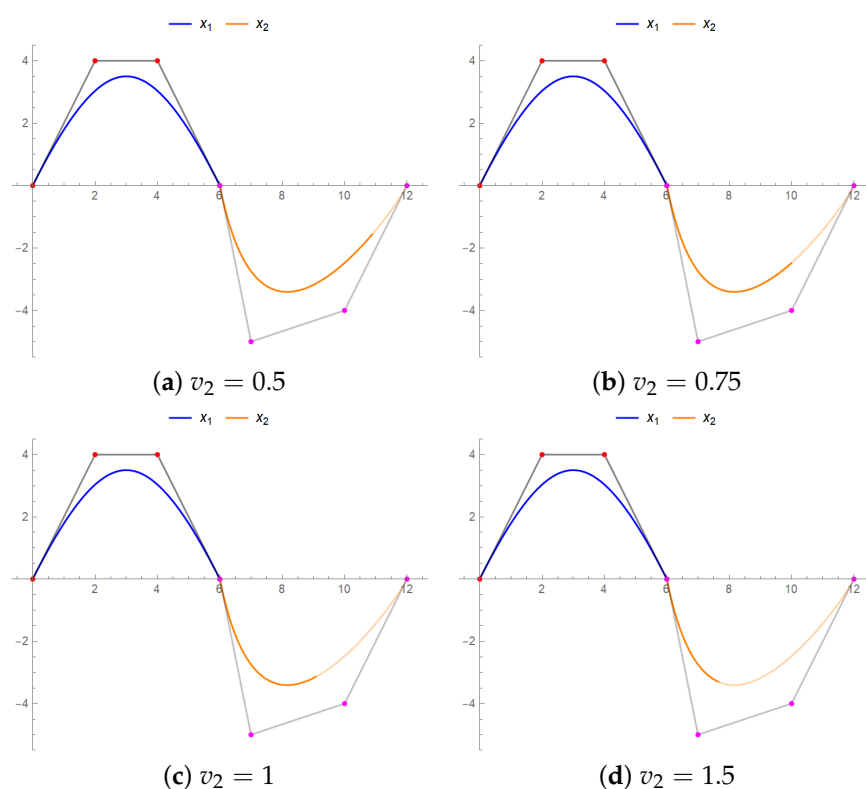


**Figure 8.**  $C^0$  continuity of two cubic fractional Bézier curves.

**Example 4.** Figure 9 shows  $C^1$  continuity for the cubic fractional Bézier curves with shape and fractional parameters variations. The control points of  $x_1$  and the shape parameters are the same as in Example 3. Likewise, the control points of  $R_0$  and  $R_1$  and can be obtained by Theorem 3, while  $R_2$  and  $R_3$  are the same as in Example 3.

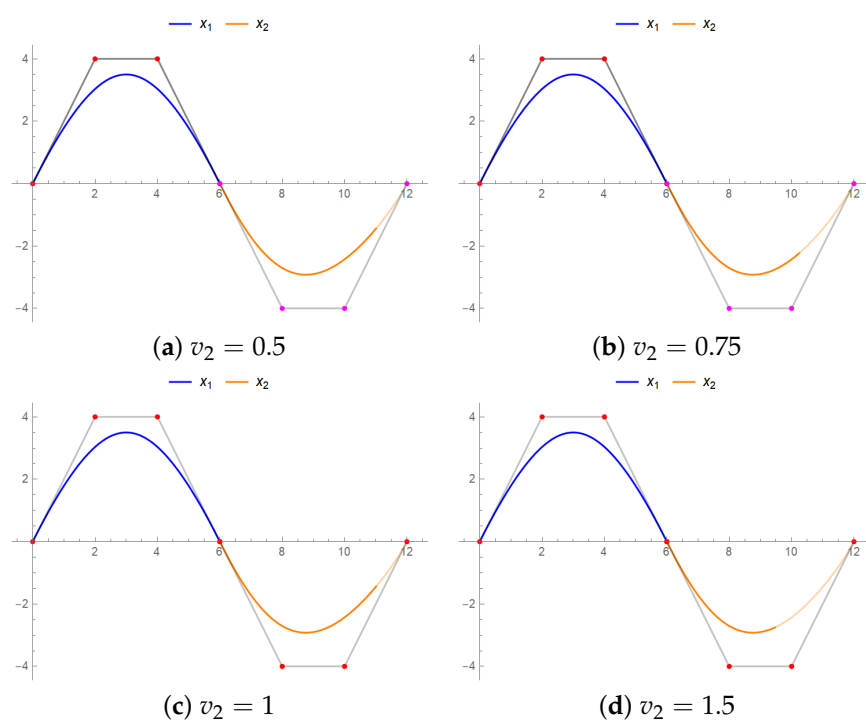


**Figure 9.**  $C^1$  continuity of two cubic fractional Bézier curves.

**Example 5.** The cubic fractional Bézier curves with variations of shape parameters and fractional parameters that satisfy the  $C^2$  continuity conditions at their joints are shown in Figure 10. The shape parameters and the control points of  $x_1$  are the same as in Example 4. By using Theorem 3, the control points of  $R_0$ ,  $R_1$  and  $R_2$  can be obtained. For the last control point,  $R_3 = (6, -12)$  is chosen.

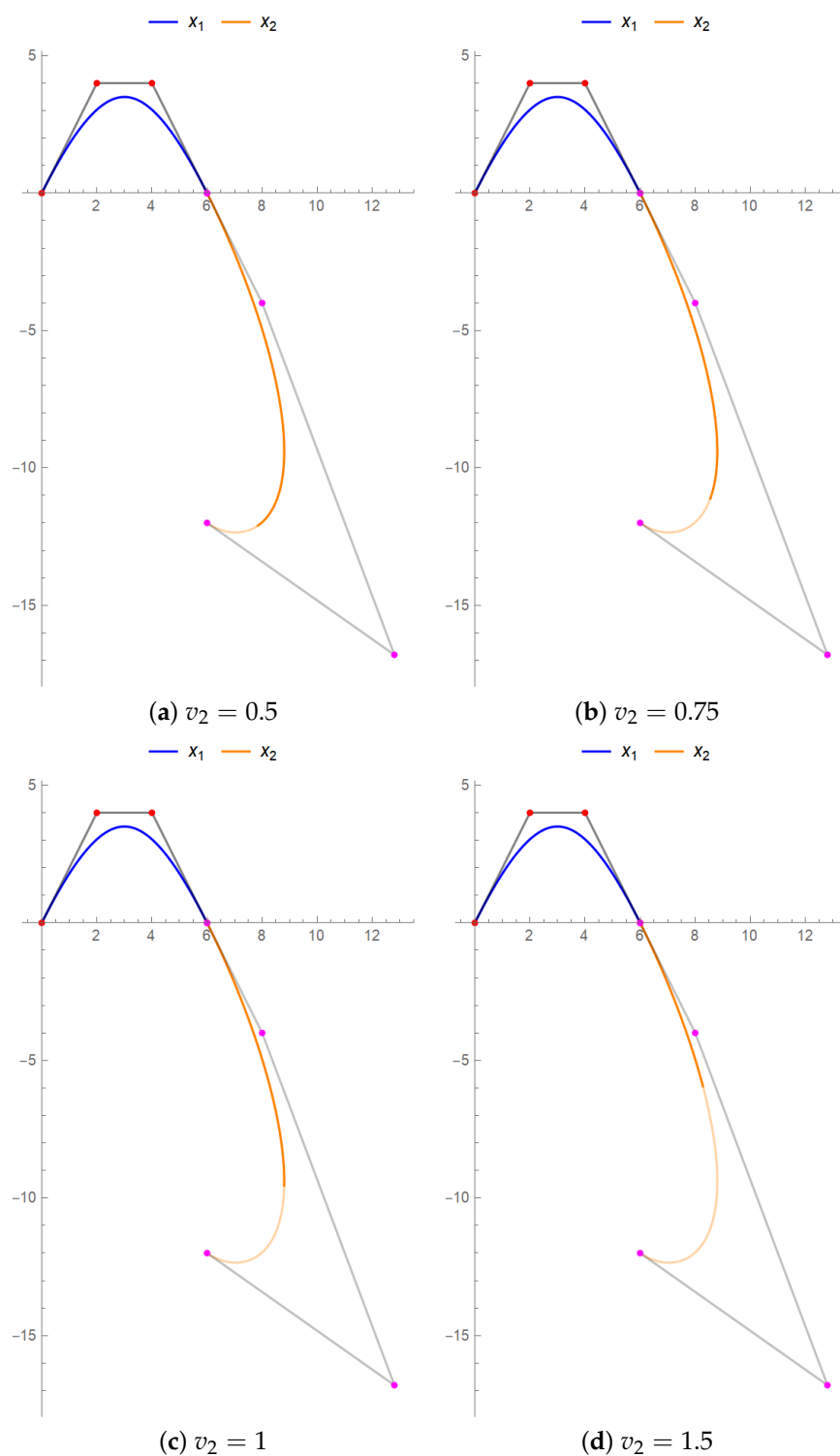


**Figure 10.**  $C^2$  continuity of two cubic fractional Bézier curves.

From Figures 9 and 10,  $C^2$  continuity is much smoother than  $C^1$  continuity. Also, from the same figures, a fraction of the second curve can be constructed by varying the fractional parameter,  $v_2$  of second curve.

#### 4.2. Geometric Continuity for Generalized Fractional Bézier Curve, $G^r$

Geometric continuity is a less restrictive form of parametric continuity. It is also independent of the parameterization but still satisfies the geometric smoothness of the resulting curve [37]. Furthermore, geometric continuity enables us to construct more shapes in less restrictive form since it has the scale factor. Hence, it is superior compared to parametric continuity [26].

**Definition 6** (General geometric continuity,  $G^r$  for curves). Consider two curves  $x_1$  on  $t \in [a, b]$  and  $x_2$  on  $t \in [a^*, b^*]$  with both curves having a degree of at least  $r + 1$ . The two curves are  $G^r$  continuous if the following conditions are satisfied:

$$\begin{aligned} x_1(b) &= x_2(a^*) \\ x'_1(b) &= \alpha_1 x'_2(a^*) \\ x''_1(b) &= \alpha_1^2 x''_2(a^*) + \alpha_2 x'_2(a^*) \\ &\vdots \\ x_1^{(r)}(b) &= \alpha_1^r x_2^{(r)}(a^*) + \alpha_2^{r-1} x_2^{(r-1)}(a^*) + \cdots + \alpha_r x'_2(a^*). \end{aligned}$$

The range of the scalar factor,  $\alpha_i$  for  $i = 0, 1, \dots, r$  depends on the degree of continuity  $r$ . Generally, for the  $G^r$  continuity, the range for the scale factors are  $\alpha_1 > 0$  and  $\alpha_i \in \mathbb{R}$  for  $i = 2, 3, \dots, r$ .

**Theorem 4** (Geometric continuity for generalized fractional Bézier curve). Consider two same degrees of generalized fractional Bézier curves as in Equations (14) and (15), the necessary and sufficient conditions for geometric continuity at the joint points, where  $v_1 = v_2 = 0$  are given by:

1.  $G^0$  continuity:

$$R_0 = Q_n. \quad (19)$$

2.  $G^1$  continuity:

$$\begin{aligned} R_0 &= Q_n, \\ R_1 &= \frac{a_n Q_{n-1} - a_n Q_n + \alpha b_1 R_0 - n Q_{n-1} + n Q_n + \alpha n R_0}{\alpha(b_1 + n)}. \end{aligned} \quad (20)$$

3.  $G^2$  continuity:

$$\begin{aligned} R_0 &= Q_n, \\ R_1 &= \frac{a_n Q_{n-1} - a_n Q_n + \alpha b_1 R_0 - n Q_{n-1} + n Q_n + \alpha n R_0}{\alpha(b_1 + n)}, \\ R_2 &= \frac{-1}{2\alpha^2(b_2 + n - 1)} \left( (n-1)(-n((-a_{n-1} + n-1)Q_{n-2} \right. \\ &\quad + (a_{n-1} + 2a_n - 2n + 2)Q_{n-1} + (-2a_n + n - 1)Q_n) + \alpha^2 n(2b_1 + n - 1)R_0 \\ &\quad \left. - \alpha^2 n(2b_1 + b_2 + 2n - 2)R_1 - \beta(b_1 + n)(R_0 - R_1) \right). \end{aligned} \quad (21)$$

**Proof.** The proof of the theorem is as follows:

1.  $G^0$  continuity is the position continuity same as  $C^0$  continuity. By solving  $x_1(1) = x_2(0)$ ,  $G^0$  continuity condition will be satisfied.

2.  $G^1$  continuity is a tangent continuity at common point but with scale factor  $\alpha$ . By solving  $x_1(1) = x_2(0)$  and  $x'_1(1) = \alpha x'_2(0)$  with  $\alpha > 0$ ,  $G^1$  continuity condition will only be satisfied when  $G^0$  continuity is satisfied.
3.  $G^0$  and  $G^1$  continuity must be satisfied first.  $G^2$  continuity is a curvature continuity at common point but with scale factors  $\alpha$  and  $\beta$ . By solving  $x_1(1) = x_2(0)$ ,  $x'_1(1) = \alpha x'_2(0)$ , and  $x''_1(1) = \alpha^2 x''_2(0) + \beta x'_2(0)$ , with  $\alpha > 0$  and  $\beta \in \mathbb{R}$ ,  $G^2$  continuity condition will be satisfied.

□

Note that when  $\alpha = 1$ , the  $G^1$  continuity will become  $C^1$  continuity. Meanwhile,  $\alpha = 1$  and  $\beta = 0$ , then  $G^2$  continuity will become  $C^2$  continuity.

**Example 6.** Figure 11 shows the cubic fractional Bézier curves with variations of fractional parameters, satisfying the  $G^1$  continuity conditions at their joints.  $x_1$  has the same control points as in Example 4. The control points of  $R_0$  and  $R_1$  and can be obtained by Theorem 4.  $R_2$  and  $R_3$  control points are arbitrarily chosen and the value  $R_2 = (10, -4)$  and  $R_3 = (12, 0)$  are chosen. Moreover,  $\alpha = 0.75$  is the scalar factor for  $\alpha > 0$ .

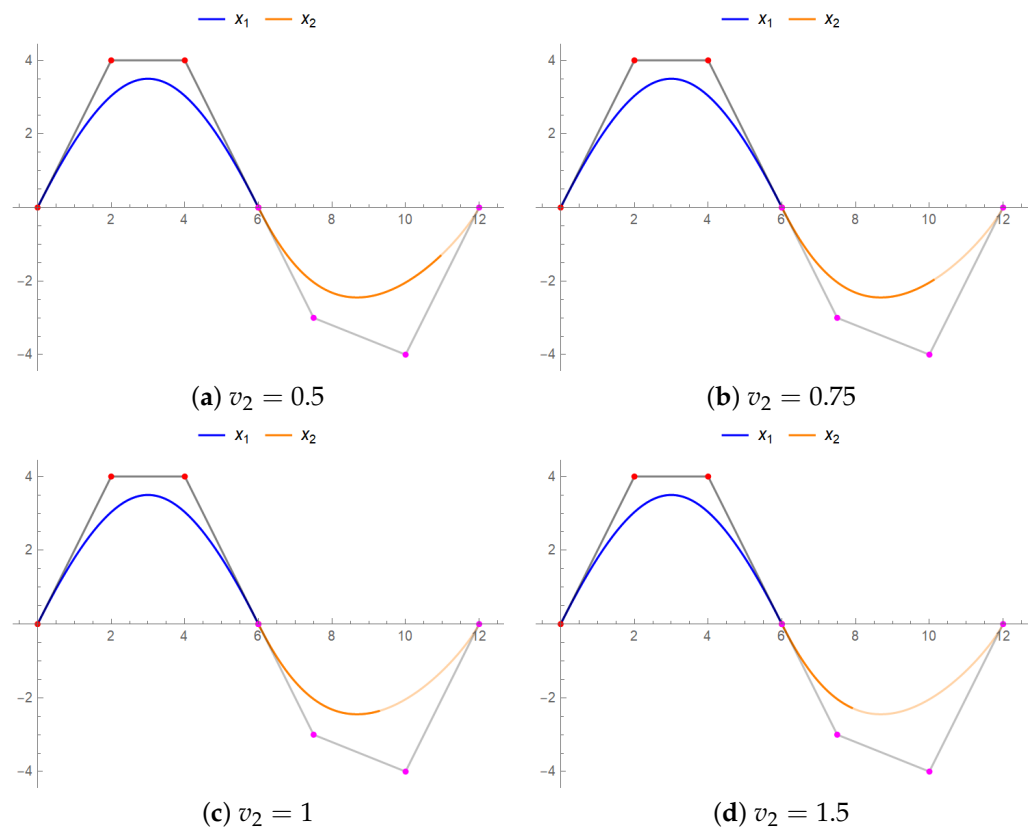


**Figure 11.**  $G^1$  continuity of two connected cubic fractional Bézier curves.

**Example 7.** The cubic fractional Bézier curves with variations of fractional parameter satisfying the  $G^2$  continuity conditions at their joints is shown in Figure 12. The control points for  $x_2$  is the same as in Example 6. By using Theorem 4, the control points of  $R_0$ ,  $R_1$  and  $R_2$  can be obtained. The last control point,  $R_3 = (6, -12)$ , is set.  $\alpha = 0.75$  and  $\beta = 0.5$  are the scalar factors, where  $\alpha > 0$  and  $\beta \in \mathbb{R}$ .

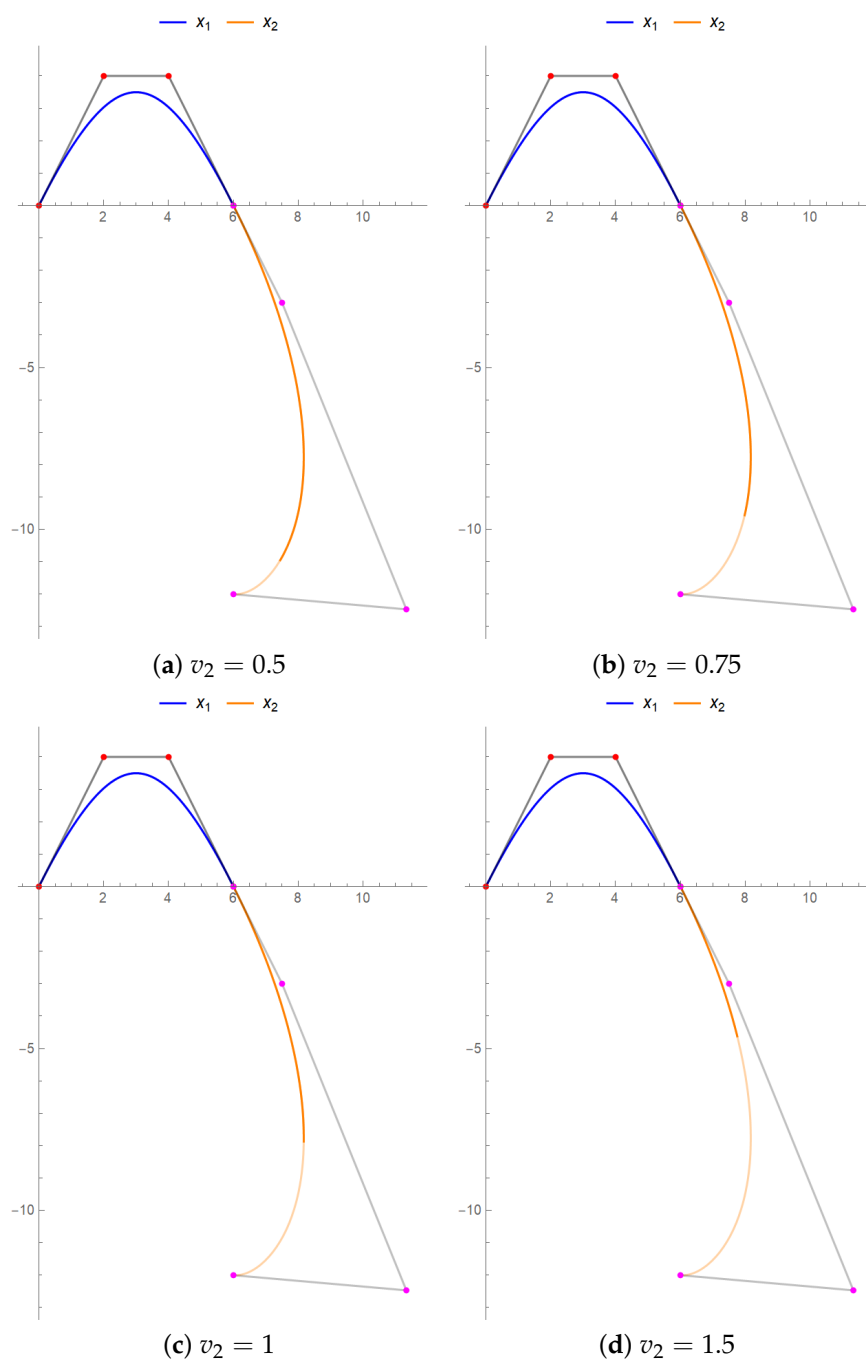


**Figure 12.**  $G^2$  continuity of two cubic fractional Bézier curves with  $\alpha$  and  $\beta$  as scaling factors.

The solid blue line represents  $x_1$ , while solid orange line represents  $x_2$  in Figures 11 and 12. Thus,  $G^2$  continuity is much smoother than  $G^1$  continuity by comparing these figures. By comparing Figures 9 and 11, the scale factor  $\alpha$  is used to control the length of the tangent. This scale factor also has the same use for  $G^2$  continuity, except that  $G^2$  continuity has one more scale factor  $\beta$ , which gives more control. Based on the Figures 9–12, the fractional parameter is used to construct the fraction of the second curve. The designer can use fractional parameter to adjust the length of the second curve. Next, we will propose a new type of continuity when the second curve of fractional Bézier can be connected at any point along the first curve.



#### 4.3. Fractional Continuity for Generalized Fractional Bézier Curve, $F^r$

The parametric and geometric continuity can be obtained by setting the value  $v_1 = 0$  for the first curve. However, if the fractional parameter  $v_1$  is not 0, the new geometric behaviour of curves that are different from the shape parameter can be seen. Therefore, by considering fractional parameter  $v_1$  into the continuity, a new type of continuity called fractional continuity will be introduced. **This type of continuity used a fractional parameter to control the position of the common point at any position along the first curve while maintaining the parametric and geometric continuity.** This fractional continuity is exclusively for the generalized fractional Bézier curve since it has the fractional parameter.

**Definition 7** (Fractional continuity for generalized fractional Bézier curve,  $F^r$ ). Consider two curves  $x_1(t; v_1)$  on  $t \in [a, b]$  and  $x_2(t; v_2)$  on  $t \in [a^*, b^*]$  with fractional parameters  $v_1$  and  $v_2$ , respectively, where both curves have a degree of at least  $r + 1$ . The two curves are  $F^r$  continuous if the following condition is satisfied:

$$\begin{aligned} x_1(b; v_1) &= x_2(a^*; 0) \\ x_1'(b; v_1) &= \alpha_1 x_2'(a^*; 0) \\ x_1''(b; v_1) &= \alpha_1^2 x_2''(a^*; 0) + \alpha_2 x_2'(a^*; 0) \\ &\vdots \\ x_1^{(r)}(b; v_1) &= \alpha_1^r x_2^{(r)}(a^*; 0) + \alpha_2^{r-1} x_2^{(r-1)}(a^*; 0) + \cdots + \alpha_r x_2'(a^*; 0). \end{aligned}$$

The range of the scalar factor,  $\alpha_i$  for  $i = 0, 1, \dots, r$  depends on the degree of continuity  $r$ . Generally, for  $F^r$  continuity, the range for the scale factors are  $\alpha_1 > 0$  and  $\alpha_i \in \mathbb{R}$  for  $i = 2, 3, \dots, r$ .

**Theorem 5** (Fractional continuity for generalized fractional Bézier curve,  $F^r$ ). Consider two same degrees of generalized fractional Bézier curves as in Equations (14) and (15), the necessary and sufficient conditions for fractional continuity at the joint points where  $v_2 = 0$  are given by:

1.  $F^0$  continuity:

$$R_0 = \sum_i^n \bar{B}_{i,n}(1; v_1, a_1, a_2, \dots, a_n) Q_i. \quad (22)$$

2.  $F^1$  continuity:

$$\begin{aligned} R_0 &= \sum_i^n \bar{B}_{i,n}(1; v_1, a_1, a_2, \dots, a_n) Q_i, \\ R_1 &= \frac{1}{\alpha(n + b_1)} \left( \frac{d}{dt} \left( \sum_i^n \bar{B}_{i,n}(t; v_1, a_1, a_2, \dots, a_n) Q_i \right)_{t=1} \right) + R_0. \end{aligned} \quad (23)$$

3.  $F^2$  continuity:

$$\begin{aligned} R_0 &= \sum_i^n \bar{B}_{i,n}(1; v_1, a_1, a_2, \dots, a_n) Q_i, \\ R_1 &= \frac{1}{\alpha(n + b_1)} \left( \frac{d}{dt} \left( \sum_i^n \bar{B}_{i,n}(t; v_1, a_1, a_2, \dots, a_n) Q_i \right)_{t=1} \right) + R_0, \\ R_2 &= \frac{1}{n + b_2 - 1} \left( \frac{1}{\alpha^2 n} \left( \frac{d^2}{dt^2} \left( \sum_i^n \bar{B}_{i,n}(t; v_1, a_1, a_2, \dots, a_n) Q_i \right)_{t=1} + \alpha(n + b_1)(R_0 - R_1) \right) \right. \\ &\quad \left. - (n + 2b_1 - 1)R_0 + (2n + 2b_1 + b_2 - 2)R_1 \right). \end{aligned} \quad (24)$$

**Proof.** The proof for the theorem is given as follows:

1.  $F^0$  continuity is the position continuity with fractional parameter  $v_1$ . By solving  $x_1(1; v_1) = x_2(0; 0)$ ,  $F^0$  continuity condition will be satisfied.
2.  $F^0$  continuity must be satisfied first.  $F^1$  continuity is a tangent continuity at common point but with scale factor  $\alpha$  and fractional parameter  $v_1$ . By solving  $x_1(1; v_1) = x_2(0; 0)$  and  $x'_1(1; v_1) = \alpha x'_2(0; 0)$  with  $\alpha > 0$ ,  $F^1$  continuity condition will be satisfied.
3.  $F^0$  and  $F^1$  continuity must be satisfied first.  $F^2$  continuity is a curvature continuity at common point but with scale factors  $\alpha$  and  $\beta$  and fractional parameter  $v_1$ . By solving  $x_1(1; v_1) = x_2(0; 0)$ ,  $x'_1(1; v_1) = \alpha x'_2(0; 0)$ , and  $x''_1(1; v_1) = \alpha^2 x''_2(0; 0) + \beta x'_2(0; 0)$ , with  $\alpha > 0$  and  $\beta \in \mathbb{R}$ ,  $F^2$  continuity condition will be satisfied.

□

Note that if  $v_1 = 0$ , then  $F^0$ ,  $F^1$  and  $F^2$  continuity, become  $G^0$ ,  $G^1$  and  $G^2$  continuity respectively. If  $v_1 = 0$  and  $\alpha = 1$ , then  $F^1$  continuity will become  $C^1$  continuity. Moreover, when  $v_1 = 0$ ,  $\alpha = 1$  and  $\beta = 0$ , then  $F^2$  continuity will become  $C^2$  continuity. For further understanding, some examples and specific corollary will be given for the cubic fractional Bézier curve.

**Corollary 1** (Fractional continuity for the cubic fractional Bézier curve). *Consider the same two degrees of cubic fractional Bézier curves as in Equations (14) and (15), the necessary and sufficient conditions for fractional continuity at the joint points, where  $v_2 = 0$ , are given by:*

1.  $F^0$  continuity:

$$R_0 = \frac{1}{2((v_1 + 1)!)^4} \left( 2Q_0((v_1 + 1)! - 1)^3((v_1 + 1)! - a_1) + Q_1((v_1 + 1)! - 1)^2(2a_1((v_1 + 1)! - 1) + 6(v_1 + 1)! - 3a_2) + 3a_2Q_2((v_1 + 1)!)^2 - 6a_2Q_2(v_1 + 1)! - 2a_3Q_2(v_1 + 1)! + 2a_3Q_3(v_1 + 1)! + 6Q_2((v_1 + 1)!)^2 - 6Q_2(v_1 + 1)! + 2Q_3(v_1 + 1)! + 3a_2Q_2 + 2a_3Q_2 - 2a_3Q_3 \right). \quad (25)$$

2.  $F^1$  continuity:

The control point for  $R_0$  is the same as  $F^0$  continuity condition.

$$R_1 = R_0 - \frac{1}{\alpha(b_1 + 3)((v_1 + 1)!)^4} \left( (v_1 + 1)(Q_0((v_1 + 1)! - 1)^2(a_1((v_1 + 1)! - 4) + 3(v_1 + 1)! - Q_1((v_1 + 1)! - 1)(a_1((v_1 + 1)!)^2 - 5(v_1 + 1)! + 4) - 3a_2((v_1 + 1)! - 2) + 3((v_1 + 1)! - 3)(v_1 + 1)! - 3a_2Q_2((v_1 + 1)!)^2 + 9a_2Q_2(v_1 + 1)! + 3a_3Q_2(v_1 + 1)! - 3a_3Q_3(v_1 + 1)! - 6Q_2((v_1 + 1)!)^2 + 9Q_2(v_1 + 1)! - 3Q_3(v_1 + 1)! - 6a_2Q_2 - 4a_3Q_2 + 4a_3Q_3) \right). \quad (26)$$

3.  $F^2$  continuity:

The control point for  $R_0$  and  $R_1$  are the same as  $F^1$  continuity condition.

$$R_2 = \frac{1}{3\alpha^2(b_2 + 2)} \left( -6\alpha^2(b_1 + 1)R_0 + 3\alpha^2(2b_1 + b_2 + 4)R_1 + \beta(b_1 + 3)(R_0 - R_1) - \frac{v_1 + 1}{((v_1 + 1)!)^4} \left( 18Q_2(v_1 + 1)! - 6Q_2((v_1 + 1)!)^2 18a_2Q_2(v_1 + 1)! - 18a_2Q_2 - 3a_2Q_2((v_1 + 1)!)^2 + 6a_3Q_2(v_1 + 1)! - 6Q_3(v_1 + 1)! - 12a_3Q_2 + 12a_3Q_3 - 6a_2Q_2v_1((v_1 + 1)!)^2 - 6a_3Q_3(v_1 + 1)! + 27a_2Q_2v_1(v_1 + 1)! + 9a_3Q_2v_1(v_1 + 1)! - 9a_3Q_3v_1(v_1 + 1)! + Q_0((v_1 + 1)! - 1)(a_1(v_1((v_1 + 1)!)^2 - 11(v_1 + 1)! + 16) - 6((v_1 + 1)! - 2)) + 3(v_1 + 1)!(v_1((v_1 + 1)! - 3) - 2) \right) \right)$$

$$\begin{aligned}
& + Q_1(-a_1((v_1 + 1)! - 1)(v_1(((v_1 + 1)!)^2 - 11(v_1 + 1)! + 16) - 6((v_1 + 1)! - 2)) \\
& + 3a_2(((v_1 + 1)!)^2 - 6(v_1 + 1)! + v_1(2((v_1 + 1)!)^2 - 9(v_1 + 1)! + 8) + 6) \\
& - 3(v_1 + 1)!(-4(v_1 + 1)! + v_1(((v_1 + 1)!)^2 - 8(v_1 + 1)! + 9) + 6)) \\
& - 12Q_2v_1((v_1 + 1)!)^2 + 27Q_2v_1(v_1 + 1)! - 9Q_3v_1(v_1 + 1)! \\
& - 24a_2Q_2v_1 - 16a_3Q_2v_1 + 16a_3Q_3v_1)) \Bigg). \tag{27}
\end{aligned}$$

By Theorem 5, all control points of  $x_1$  are used in fractional continuity to determine the control points for  $x_2$ . The fractional parameter  $v_2 = 0$  does not affect the endpoint of  $x_2$  at  $t = 0$ . This is because, for  $t = 0$ ,  $x_2$  does not depend on  $v_2$ . Hence, to simplify the calculation,  $v_2 = 0$  is substituted to the Theorem 5.

**Example 8.** Figure 13 shows two cubic fractional Bézier curves connected with  $F^0$  continuity. The control points for  $x_1$  are  $Q_0 = (0, 0)$ ,  $Q_1 = (2, 4)$ ,  $Q_2 = (4, 4)$  and  $Q_3 = (6, 0)$  with shape parameters  $(a_1, a_2, a_3) = (1, 0, -1)$ . For  $x_2$ , the first control point (common point) can be obtained using Theorem 5. The other control points for  $x_2$  are  $R_1 = (7, -5)$ ,  $R_2 = (10, -4)$  and  $R_3 = (12, 0)$  with shape parameters  $(b_1, b_2, b_3) = (1, 0.75, 2)$ . The opacity lines is representation of continuity of curves when  $v_1 = v_2 = 0$ . The solid lines indicate the behavior of the fractional continuity at various value of  $v_1$  and  $v_2$ . This representation is similar to that in Examples 9 and 10.

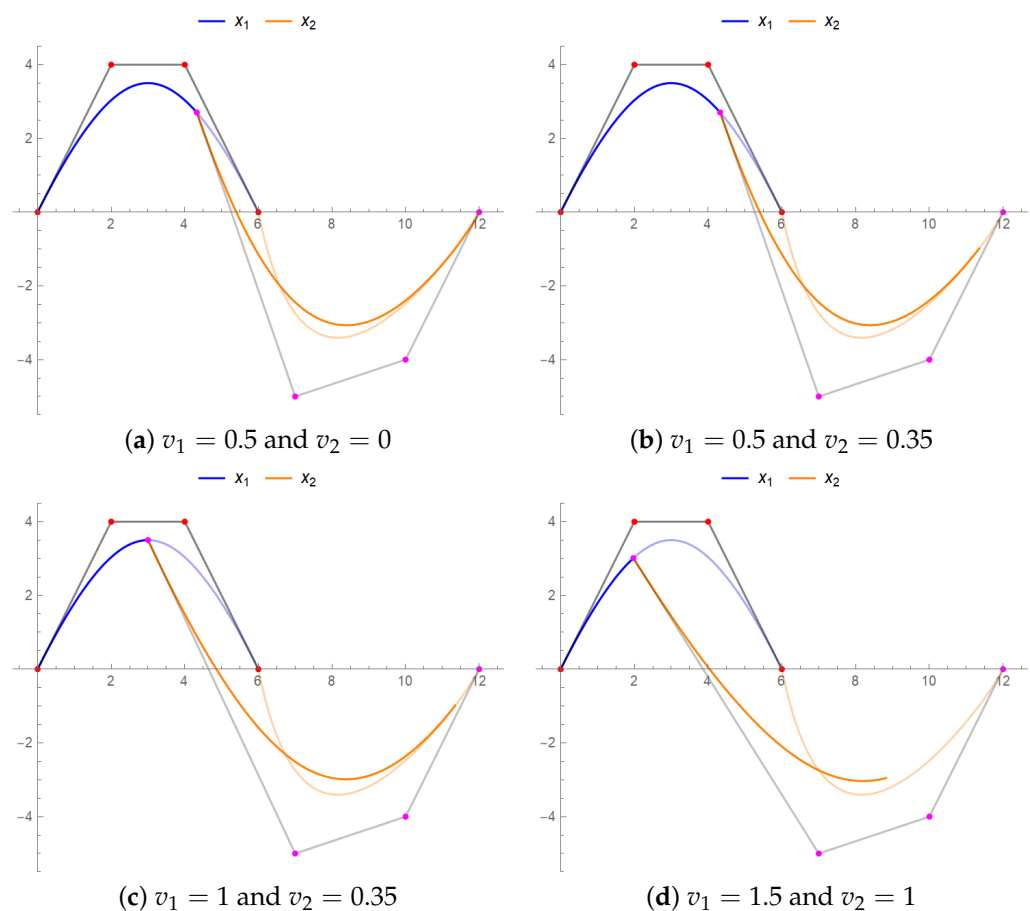
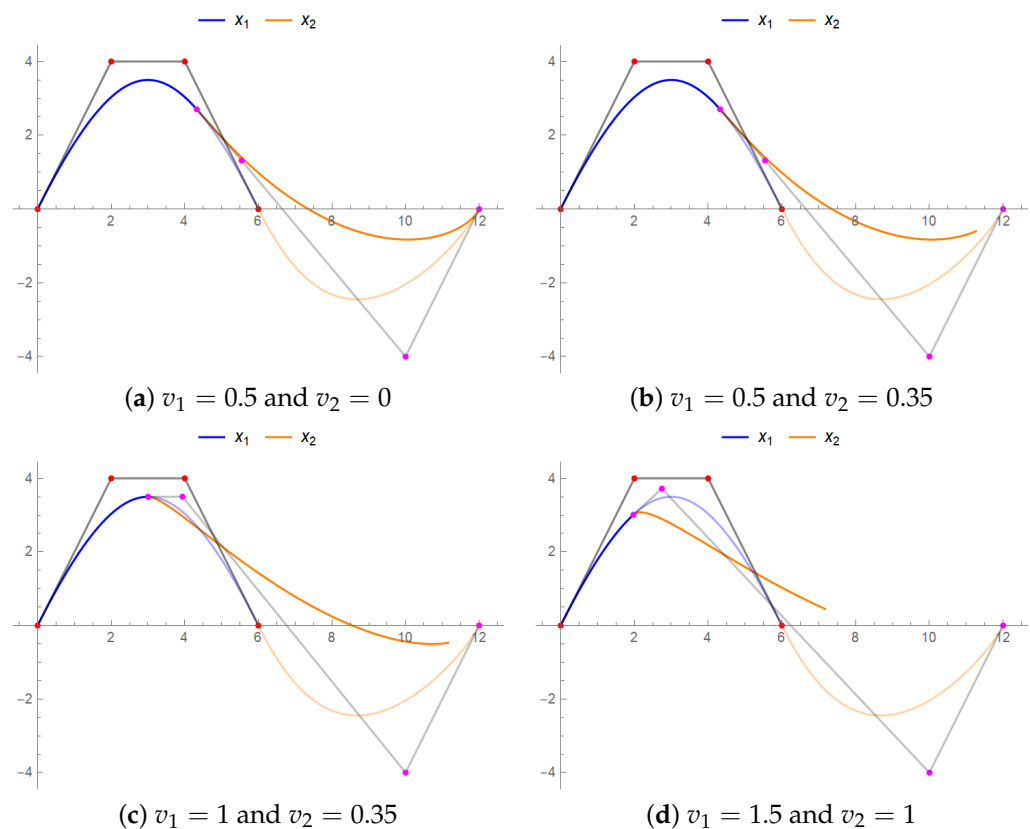


Figure 13.  $F^0$  continuity with multiple values of  $v_1$  and  $v_2$ .

**Example 9.** Two cubic fractional Bézier curves connected with  $F^1$  continuity with  $\alpha = 0.75$  are shown in Figure 14. The control points and shape parameters for  $x_1$  are similar to Example 8. The first and second control point of  $x_2$  can be obtained using Theorem 5. The rest control points and shape parameters for  $x_2$  are the same as Example 8.



**Figure 14.**  $F^1$  continuity with multiple values of  $v_1$  and  $v_2$ .

**Example 10.** Two cubic fractional Bézier curves connected with  $F^2$  continuity with  $\alpha = 0.75$  and  $\beta = 0.5$  are shown in Figure 15. The control points and shape parameters for  $x_1$  are the same as Example 8. By using Theorem 5, the first, second and third control points of  $x_2$  can be obtained. The shape parameters for  $f_1$  is similar to Example 9. For the last control point for  $x_1$ ,  $R_3 = (6, -12)$  is chosen.

From Figures 13–15, fractional parameter  $v_1$  changes the common point position along the  $x_1$  but still maintains the continuity. Thus, the common point moves along the curve  $x_1$  by changing the value of fractional parameter  $v_1$ . This fractional parameter gives the designer more control of the curve in terms of length adjustability. Moreover, the shape parameter gives more flexibility control to the designer to vary the shapes and still maintain their geometrical properties.

From the same figures, the fractional parameter  $v_2$  does not affect the continuity of the two curves at the common point. When  $t = 0$ , the curve  $x_2$  is reduced to the terms without the fractional parameter  $v_2$ . Hence, in the Definition 7, the value of  $v_2 = 0$  is used to simplify the calculation of the formula calculation. For all types of continuity, the control points of the second curve are derived from all the control points of the first curve  $x_1$  using Theorem 5.

There is an alternative way of constructing a fraction of the curve, which is by varying the domain of  $t$ . However, there is a limitation in using this method where the domain of  $t$  needs to be fixed. The fractional parameter overcomes this limitation and maintains the domain of  $t$  at  $[0, 1]$ . Surprisingly, when this fractional parameter is used in continuity, a new type continuity can be derived, which may be reduced to parametric and geometric continuity.

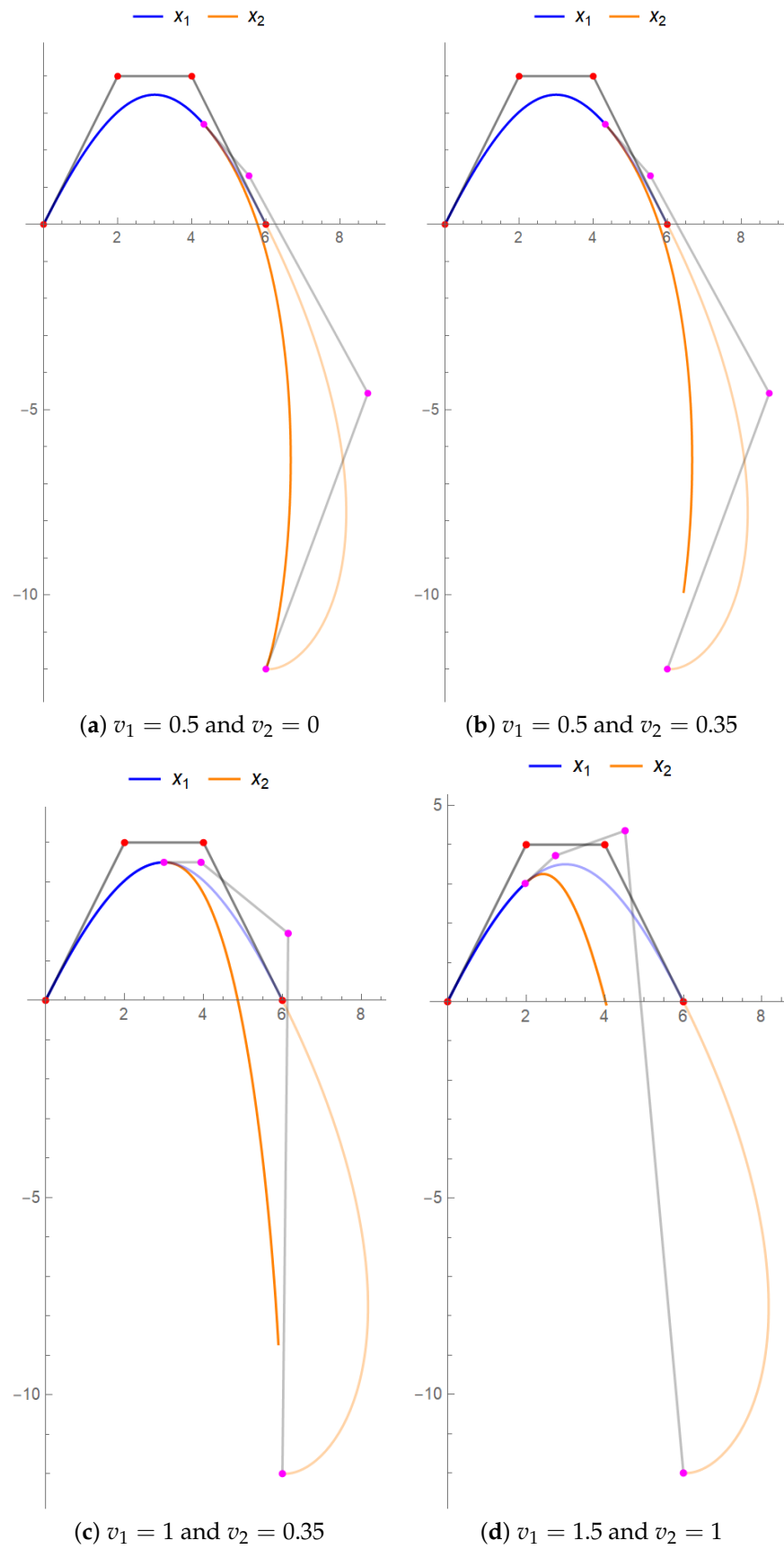
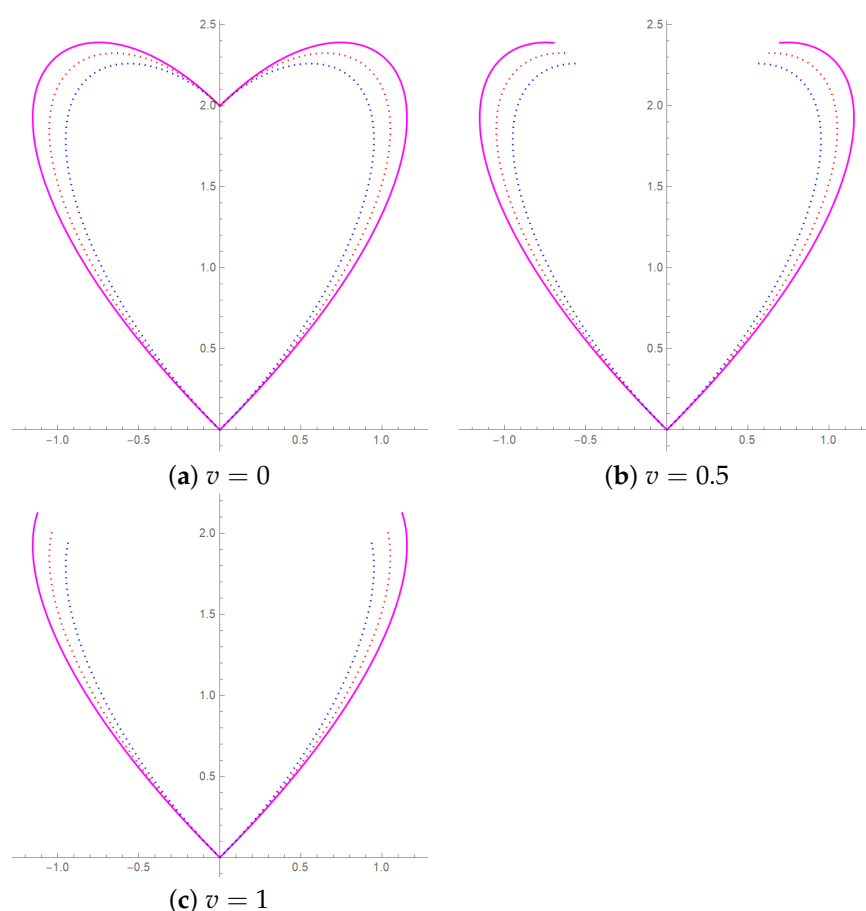


Figure 15.  $F^2$  continuity with multiple values of  $v_1$  and  $v_2$ .

### 5. Modelling of Shapes Using Generalized Fractional Bézier Curves

In the world we live in, numerous fascinating shapes occurred through natural phenomena. These fascinating natural shapes motivate scholars to analyse the shapes and determine their mathematical representation. In this section, some shapes are modelled using the generalized fractional Bézier curves with shape parameters.

**Example 11.** Figure 16 shows the modelling shape of the heart using cubic fractional Bézier curves. Two curves,  $f_1$  and  $f_2$ , are connected at starting points  $(0,0)$  and  $(0,2)$  at the endpoint. The intermediate point for  $f_1$  are  $(2,2)$  and  $(1,3)$ , and for  $f_2$  are  $(-2,2)$  and  $(-1,3)$ . Figure 16 shows three different shapes with different values of shape and fractional parameters. The shape parameters used are  $(0,0,0)$ ,  $(0.5,0,-0.5)$  and  $(1,0,-1)$  for the magenta, red, and blue curves respectively. Different states of shape can be modelled when you change the values of the fractional parameter, as shown in Figure 16a–c.



**Figure 16.** Modelling shape of heart using cubic fractional Bézier curve with different shape parameters and fractional parameter.

**Example 12.** The cubic fractional Bézier curves are used to model the shape of a petal. Here, four curves of cubic fractional Bézier are used to model the petal, as shown in Figure 17.



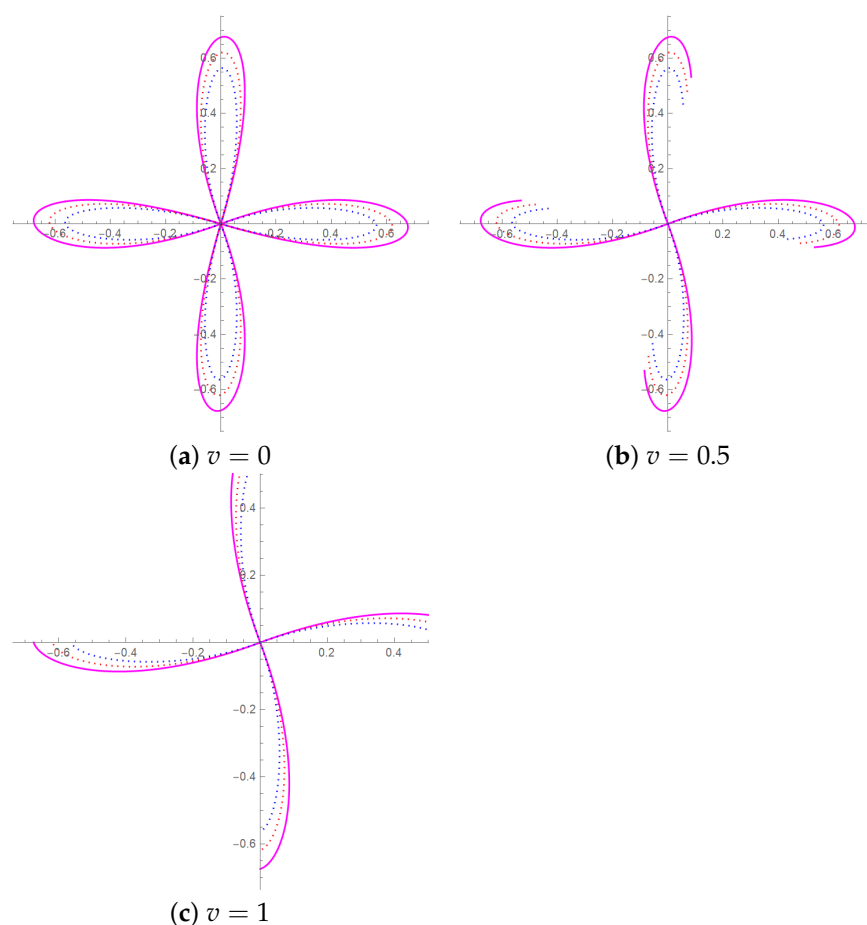


**Figure 17.** Modelling shape of petal using cubic fractional Bézier curve with different shape parameters and fractional parameter.

## 6. Construction of Surface Using Generalized Fractional Bézier Curve

Surfaces can be generated by using curves. For example, some surfaces can be generated by revolving around an axis, while others can be generated by extruding the curve along a scalar vector. In this section, some examples of simple types of surfaces are presented.

### 6.1. Surface Revolution

From the constructed curve, a surface can be generated by rotating the constructed curve about an axis. The resulting surface always has azimuthal symmetry called the surface revolution along the particular axis. In this work, the surface is generated using two connected cubic fractional Bézier curves. The two cubic fractional Bézier curves are defined as follows.

$$f_1(t; v_1, a_1, a_2, a_3) = \sum_{i=0}^3 \bar{F}_{i,3}(t; v_1, a_1, a_2, a_3) P_i, \quad t \in [0, 1], \quad (28)$$

$$f_2(t; v_2, b_1, b_2, b_3) = \sum_{j=0}^3 \bar{F}_{j,3}(t; v_2, b_1, b_2, b_3) Q_j, \quad t \in [0, 1], \quad (29)$$

where  $P_i$  and  $Q_i$  for  $i = 0, 1, 2, 3$  are the control points. The shape parameters  $a_1, a_2, a_3$  and  $b_1, b_2, b_3$  are for curves  $f_1$  and  $f_2$ , respectively, while the fractional parameters  $v_1$  and  $v_2$  are for curves  $f_1$  and  $f_2$ , respectively. Note that the two curves are connected at  $t = 0$ . The surface revolution is constructed by rotating the curves defined in Equations (28) and (29) through the  $x$ -axis.

**Example 13.** The control points of the two connected curves are  $P_0 = Q_0 = (0, 2)$ ,  $P_1 = (-3, 3)$ ,  $P_2 = (-6, 3)$ ,  $P_3 = (-7, 2)$ ,  $Q_1 = (4, 5)$ ,  $Q_2 = (10, 3)$  and  $Q_3 = (8, 0)$ . Figure 18 shows the surface revolution constructed with shape parameters with the values of  $a_1 = a_2 = a_3 = b_1 = b_2 = b_3 = 0$  with multiple values of fractional parameters  $v_1$  and  $v_2$ . The surface with low opacity is the classical Bézier surface generated when  $v = 0$ .

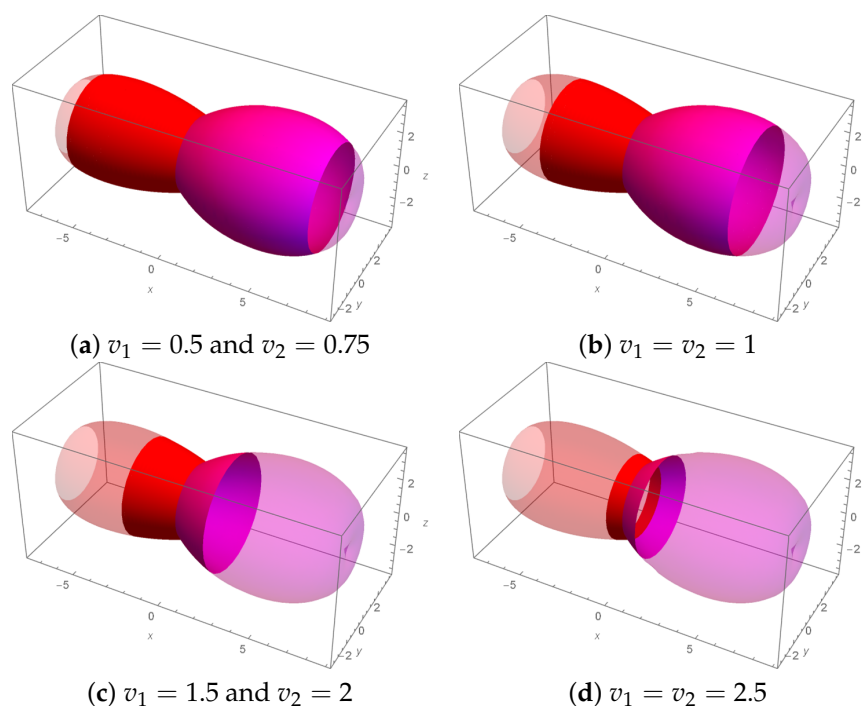


**Figure 18.** Surface revolution at x-axis of two connected cubic fractional Bézier curves.

**Example 14.** The control points of the two connected curves are the same as in Figure 18. Surface revolution is constructed with shape parameters with the values of  $a_1 = -2.5$ ,  $a_2 = 2$ ,  $a_3 = -1$ ,  $b_1 = 1$ ,  $b_2 = -1$ , and  $b_3 = 2$  with multiple values of fractional parameters  $v_1$  and  $v_2$  as in Figure 19. The red surface is generated by curve  $f_1$ , while the blue surface is generated by curve  $f_2$ . Note that by varying the fractional parameters  $v_1$  and  $v_2$  values, the fraction of the curve can be controlled. The shape parameters will further assist in controlling the shape of the surface. At  $v = 0$ , the Bézier surface with shape parameters is generated using low opacity.

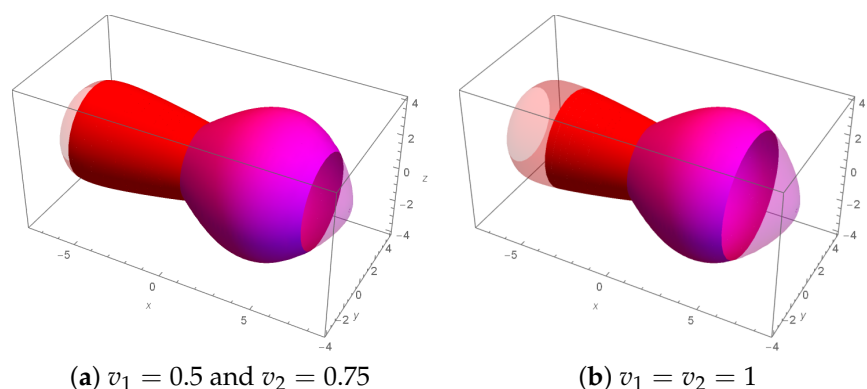


**Figure 19.** Cont.

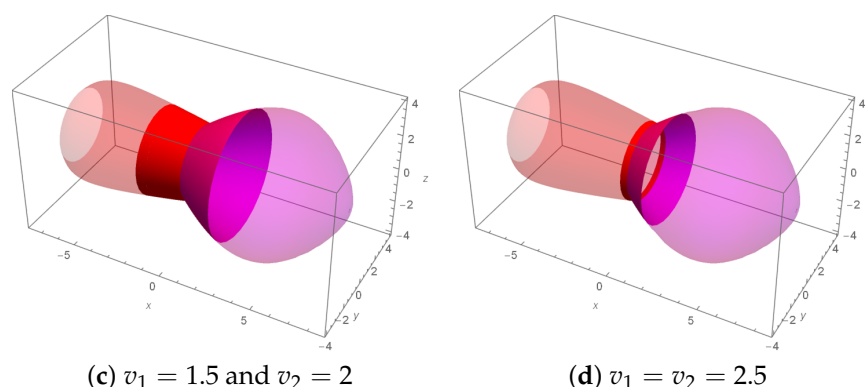


**Figure 19.** Surface revolution of  $x$ -axis of two connected cubic fractional Bézier curves with different shape parameters.

### 6.2. Extruded Surface

The extruded surface is a surface generated when a curve is extruded along a scalar vector. For example, let  $f(u)$  be the parametric curve in  $u$  direction with  $u \in [0, 1]$ , then the extruded surface  $S(u, v)$  is defined as follows.

$$S(u, v) = f(u) + v\mathbf{a}, \quad (30)$$

where  $\mathbf{a}$  is vector and  $v \in [0, \alpha]$  with  $\alpha \in \mathbb{R}$  is a scalar.

**Example 15.** Figure 20 shows an extruded surface is generated by cubic fractional Bézier curve with control points  $P_0 = (0, 0, -1)$ ,  $P_1 = (2, 2, -2)$ ,  $P_2 = (4, -2, -3)$  and  $P_3 = (6, 0, 0)$ , fractional parameter  $v$  and shape parameters  $a_1 = a_2 = a_3 = 0$  with the vector  $\mathbf{a} = \langle 0, 3, 2 \rangle$ . The low opacity surface is the extruded classical Bézier surface with  $v = 0$ .

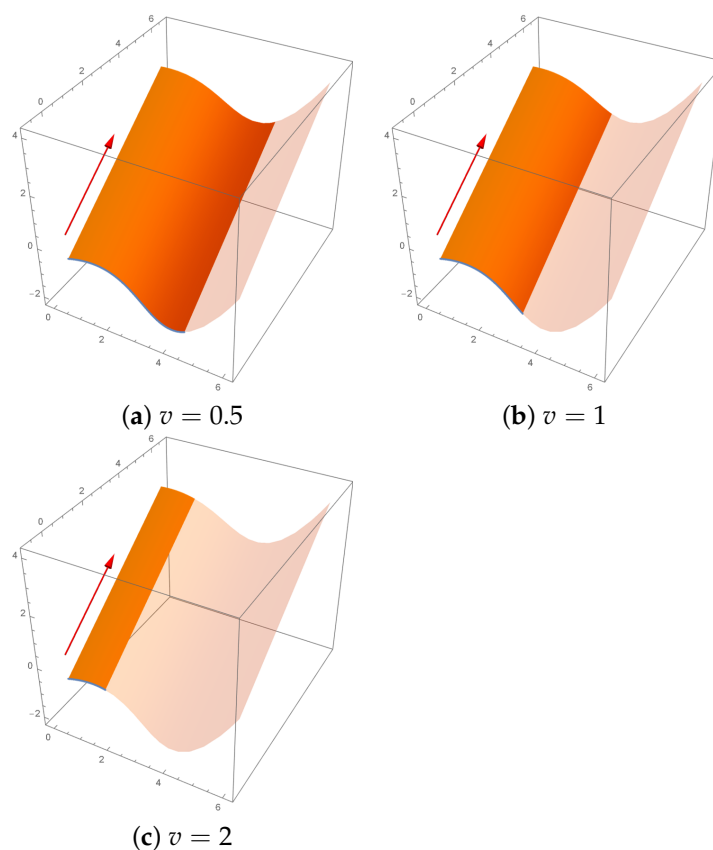


**Figure 20.** Extruded surface generated by cubic fractional Bézier curves with different fractional parameter.

**Example 16.** Figure 21 shows extruded surface generated by a cubic fractional Bézier curve with same control points in Figure 20 with fractional parameter  $v$  and shape parameters  $a_1 = 0.5$ ,  $a_2 = -1$  and  $a_3 = 2$  with the vector  $\mathbf{a} = \langle 1, 2, 1 \rangle$ . The blue line is the curve, while the red arrow line is the vector in Figures 20 and 21. The low opacity surface is the extruded Bézier surface with  $v = 0$  and shape parameters, as stated above.

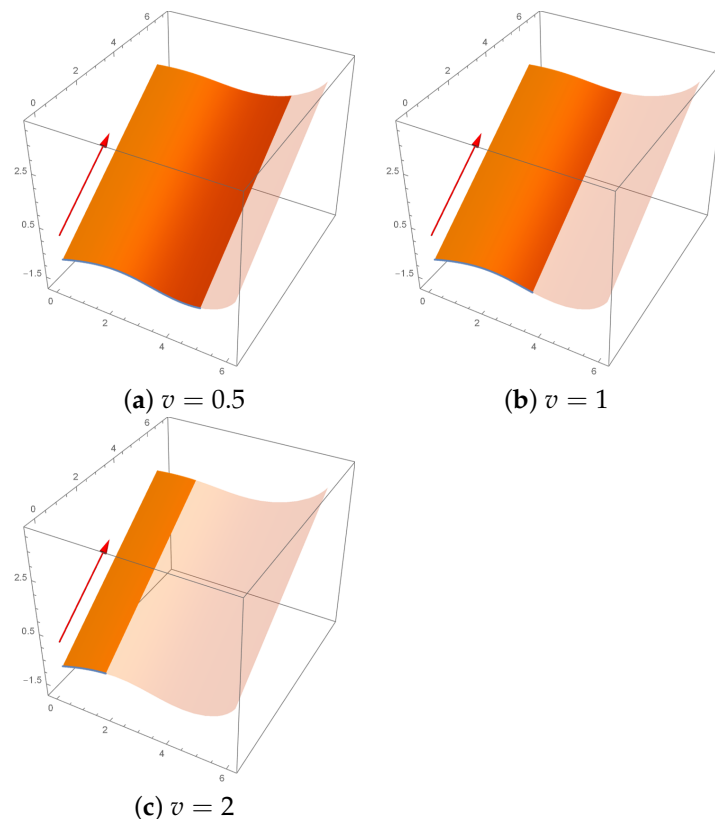


**Figure 21.** Extruded surface generated by cubic fractional Bézier curves with different fractional parameter.

## 7. Conclusions

Applying the Riemann-Liouville fractional integral in constructing a new type of Bézier curve creates two different sets of parameters called the shape and fractional parameter. The shape parameters provide flexibility to alter the shape of the curve by retaining the existing control points. In contrast, the fractional parameter provides elasticity of controlling the optimal length of the curve. All the properties of the fractional Bézier curve resemble the basic properties of the Bézier curve. **The generalized fractional Bézier curve satisfies all the properties of the Bézier curve, which can be reverted to the original Bézier curve when the fractional parameter is  $v = 0$ .** The generalized fractional Bézier curve's flexibility and elasticity is the dominant advantage for this new type of Bézier basis function, especially in path and trajectory problems. The overshooting issue that occurs in curve fitting is overcome by applying the basis functions.

A new type of continuity called fractional continuity is one of the main advantages of using the basis functions. This fractional continuity enables the constructed curves to change their common point while maintaining their continuity. Furthermore, this fractional parameter offers more control of a curve to be connected with another curve considering particular points along the curve. Usually, using parametric continuity and geometric continuity, the designer has to change the control points and calculate the control points again if the designer wants to connect the curve at a particular point on the same curve. However, this fractional continuity will be more effective and convenient because varying the fractional parameter of the first curve can connect with the second curve at any point

on the first curve. For future research, this work can be extended to discuss the modelling of generalized fractional Bézier surfaces, such as tensor product surface, ruled surface, and coon patch.

**Author Contributions:** Conceptualization, M.Y.M.; Validation, K.T.M.; writing—original draft preparation, S.A.A.A.S.M.Z.; formal analysis, S.A.A.A.S.M.Z.; visualization, S.A.A.A.S.M.Z.; supervision, M.Y.M. All authors have read and agreed to the published version of the manuscript.

**Funding:** Ministry of Higher Education Malaysia through Fundamental Research Grant Scheme (FRGS/1/2020/STG06/USM/03/1) and School of Mathematical Sciences, Universiti Sains Malaysia.

**Acknowledgments:** This research is supported by the Ministry of Higher Education Malaysia through Fundamental Research Grant Scheme (FRGS/1/2020/STG06/USM/03/1) and School of Mathematical Sciences, Universiti Sains Malaysia. The authors are very grateful to the anonymous referees for their valuable suggestions.

**Conflicts of Interest:** The authors declare no conflict of interest.

## References

1. Prautzsch, H.; Boehm, W.; Paluszny, M. *Bézier and B-Spline Techniques*; Springer Science & Business Media: Berlin/Heidelberg, Germany, 2002.
2. Farin, G.E.; Farin, G. *Curves and Surfaces for CAD: A Practical Guide*; Morgan Kaufmann: Burlington, MS, USA, 2002.
3. Yang, L.; Zeng, X.M. Bézier curves and surfaces with shape parameters. *Int. J. Comput. Math.* **2009**, *86*, 1253–1263. [\[CrossRef\]](#)
4. Wang, W.T.; Wang, G.Z. Bézier curves with shape parameter. *J. Zhejiang Univ. Sci. A* **2005**, *6*, 497–501.
5. Dube, M.; Sharma, R. Quartic trigonometric Bézier curve with a shape parameter. *Int. J. Math. Comput. Appl. Res.* **2013**, *3*, 89–96.
6. Han, X.A.; Ma, Y.; Huang, X. The cubic trigonometric Bézier curve with two shape parameters. *Appl. Math. Lett.* **2009**, *22*, 226–231. [\[CrossRef\]](#)
7. Misro, M.Y.; Ramli, A.; Ali, J.M. Quintic trigonometric Bézier curve with two shape parameters. *Sains Malays.* **2017**, *46*, 825–831.
8. Misro, M.Y.; Ramli, A.; Ali, J.M.; Abd Hamid, N.N. Cubic trigonometric Bézier spiral curves. In Proceedings of the 2017 14th International Conference on Computer Graphics, Imaging and Visualization, Marrakesh, Morocco, 23–25 May 2017; pp. 14–20.
9. Misro, M.Y.; Ramli, A.; Ali, J.M. Extended analysis of dynamic parameters on cubic trigonometric Bézier transition curves. In Proceedings of the 2019 23rd International Conference in Information Visualization—Part II, Paris, France, 2–5 July 2019; pp. 141–146.
10. Misro, M.Y.; Ramli, A.; Ali, J.M.; Abd Hamid, N.N. Pythagorean hodograph quintic trigonometric Bézier transition curve. In Proceedings of the 2017 14th International Conference on Computer Graphics, Imaging and Visualization, Marrakesh, Morocco, 23–25 May 2017; pp. 1–7.
11. Misro, M.Y.; Ramli, A.; Ali, J.M. Quintic trigonometric Bézier curve and its maximum speed estimation on highway designs. In *AIP Conference Proceedings*; AIP Publishing LLC: Melville, NY, USA, 2018; p. 020089.
12. Yan, Z.; Schiller, S.; Wilensky, G.; Carr, N.; Schaefer, S. K-curves: Interpolation at local maximum curvature. *Acm Trans. Graph. (TOG)* **2017**, *36*, 1–7. [\[CrossRef\]](#)
13. Yuksel, C. A Class of C2 Interpolating Splines. *Acm Trans. Graph. (TOG)* **2020**, *39*, 1–14. [\[CrossRef\]](#)
14. Adnan, S.B.Z.; Ariffin, A.A.M.; Misro, M.Y. Curve fitting using quintic trigonometric Bézier curve. In *AIP Conference Proceedings*; AIP Publishing LLC: Melville, NY, USA, 2020; Volume 2266, p. 040009.
15. Piegl, L.; Tiller, W. Curve and surface constructions using rational B-splines. *Comput. Aided Des.* **1987**, *19*, 485–498. [\[CrossRef\]](#)
16. Dimas, E.; Briassoulis, D. 3D geometric modelling based on NURBS: A review. *Adv. Eng. Softw.* **1999**, *30*, 741–751. [\[CrossRef\]](#)
17. Barbat, C.S. Examples of Bézier-Surfaces of Revolution. *J. Geom. Graph.* **2005**, *9*, 1–9.
18. Ismail, N.H.M.; Misro, M.Y. Surface construction using continuous trigonometric Bézier curve. In *AIP Conference Proceedings*; AIP Publishing LLC: Melville, NY, USA, 2020; p. 040012.
19. Ammad, M.; Misro, M.Y. Construction of Local Shape Adjustable Surfaces Using Quintic Trigonometric Bézier Curve. *Symmetry* **2020**, *12*, 1205. [\[CrossRef\]](#)
20. DeRose, T.D.; Barsky, B.A. An intuitive approach to geometric continuity for parametric curves and surfaces. In *Computer-Generated Images*; Springer: Berlin/Heidelberg, Germany, 1985; pp. 159–175.
21. Ziatdinov, R.; Yoshida, N.; Kim, T.w. Fitting G2 multispiral transition curve joining two straight lines. *Comput. Aided Des.* **2012**, *44*, 591–596. [\[CrossRef\]](#)
22. Barsky, B.A.; DeRose, T.D. Geometric continuity of parametric curves: Constructions of geometrically continuous splines. *IEEE Comput. Graph. Appl.* **1990**, *10*, 60–68. [\[CrossRef\]](#)
23. Qin, X.; Hu, G.; Zhang, N.; Shen, X.; Yang, Y. A novel extension to the polynomial basis functions describing Bézier curves and surfaces of degree n with multiple shape parameters. *Appl. Math. Comput.* **2013**, *223*, 1–16. [\[CrossRef\]](#)
24. Bashir, U.; Abbas, M.; Ali, J.M. The G2 and C2 rational quadratic trigonometric Bézier curve with two shape parameters with applications. *Appl. Math. Comput.* **2013**, *219*, 10183–10197. [\[CrossRef\]](#)

- 
25. Hu, G.; Bo, C.; Qin, X. Continuity conditions for Q-Bézier curves of degree  $n$ . *J. Inequal. Appl.* **2017**, *2017*, 1–14. [[CrossRef](#)]
  26. BiBi, S.; Abbas, M.; Miura, K.T.; Misro, M.Y. Geometric Modeling of Novel Generalized Hybrid Trigonometric Bézier-Like Curve with Shape Parameters and Its Applications. *Mathematics* **2020**, *8*, 967. [[CrossRef](#)]
  27. Miller, K.S.; Ross, B. *An Introduction to the Fractional Calculus and Fractional Differential Equations*; Wiley: Hoboken, NJ, USA, 1993.
  28. Samko, S.G.; Kilbas, A.A.; Marichev, O.I. *Fractional Integrals and Derivatives*; Gordon and Breach Science Publishers: Yverdon Yverdon-les-Bains, Switzerland, 1993; Volume 1.
  29. Baleanu, D.; Güvenç, Z.B.; Machado, J.T. *New Trends in Nanotechnology and Fractional Calculus Applications*; Springer: Berlin/Heidelberg, Germany, 2010.
  30. Iqbal, S.; Mubeen, S.; Tomar, M. On Hadamard  $k$ -fractional integrals. *J. Fract. Calc. Appl.* **2018**, *9*, 255–267.
  31. Caputo, M. Linear models of dissipation whose  $Q$  is almost frequency independent—II. *Geophys. J. Int.* **1967**, *13*, 529–539. [[CrossRef](#)]
  32. Alqahtani, R.T. Atangana-Baleanu derivative with fractional order applied to the model of groundwater within an unconfined aquifer. *J. Nonlinear Sci. Appl.* **2016**, *9*, 3647–3654. [[CrossRef](#)]
  33. Li, X. Numerical solution of fractional differential equations using cubic B-spline wavelet collocation method. *Commun. Nonlinear Sci. Numer. Simul.* **2012**, *17*, 3934–3946. [[CrossRef](#)]
  34. Arshed, S. Quintic B-spline method for time-fractional superdiffusion fourth-order differential equation. *Math. Sci.* **2017**, *11*, 17–26. [[CrossRef](#)]
  35. Ghomanjani, F. A numerical technique for solving fractional optimal control problems and fractional Riccati differential equations. *J. Egypt. Math. Soc.* **2016**, *24*, 638–643. [[CrossRef](#)]
  36. Misro, M.Y.; Ramli, A.; Hoe, L.K. Determining degree of road elevation using spatial Bézier curve. In *AIP Conference Proceedings*; AIP Publishing LLC: Melville, NY, USA, 2019; Volume 2184, p. 060043.
  37. Barsky, B.A.; DeRose, T.D. Geometric continuity of parametric curves: Three equivalent characterizations. *IEEE Comput. Graph. Appl.* **1989**, *9*, 60–69. [[CrossRef](#)]